Pisias, N.G., Mayer, L.A., Janecek, T.R., Palmer-Julson, A., and van Andel, T.H. (Eds.), 1995
*Proceedings of the Ocean Drilling Program, Scientific Results,* Vol. 138

# 3. REFINEMENT OF A HIGH-RESOLUTION, CONTINUOUS SEDIMENTARY SECTION FOR STUDYING EQUATORIAL PACIFIC OCEAN PALEOCEANOGRAPHY, LEG 138[1]

T.K. Hagelberg,[2,3] N.G. Pisias,[2] N.J. Shackleton,[4] A.C. Mix,[2] and S. Harris[2]

**ABSTRACT**

Ocean Drilling Program (ODP) Leg 138 was designed to study the late Neogene paleoceanography of the equatorial Pacific Ocean at time scales of thousands to millions of years. Crucial to this objective was the acquisition of continuous, high-resolution sedimentary records. It is well known that between successive advanced piston corer (APC) cores, portions of the sedimentary sequence often are absent, despite the fact that core recovery is often recorded as 100%. To confirm that a continuous sedimentary sequence was sampled, each of the 11 drill sites was multiple-APC-cored. At each site, continuously measured records of magnetic susceptibility, gamma-ray attenuation porosity evaluator (GRAPE), wet-bulk density, and digital color reflectance were used to monitor section recovery. These data were used to construct a composite depth section while at the site. This strategy often verified 100% recovery of the complete sedimentary sequence with two or three offset piston-cored holes.

Here, these initial efforts have been extended to document the recovery of a complete sediment section and to investigate sources of error associated with sediment density measurements and changes in local sedimentation rates. At Sites 846 through 852, fine-scale correlation (on the order of centimeters) of the GRAPE records was accomplished using the inverse correlation techniques of Martinson et al. (1982). Having a common depth scale for all holes at each site facilitated comparison of high-resolution data from different holes. After refining the interhole correlation, GRAPE records from adjacent holes were "stacked" to produce a less noisy estimate of sediment wet-bulk density for Sites 846 through 852. The continuity of the stacked GRAPE record is confirmed with reflectance and susceptibility records. The resulting stacked GRAPE records have a temporal resolution of less than 1000 yr for the past 5 m.y. Moreover, the stacking procedure allows for development of error estimates for measurements present in more than one hole. An important advantage provided by this framework is that one can determine the range of sedimentation variability between adjacent holes at a given site. This variability is caused by local sedimentation variability and by artifacts of the coring process. We demonstrate that the depth domain changes in sedimentation variability required to correlate among adjacent holes are larger than the changes induced by time-scale tuning procedures.

## INTRODUCTION

The primary objective of Leg 138 was the acquisition of high-resolution records of late Neogene climatic variability from the eastern equatorial Pacific Ocean (Mayer, Pisias, Janecek, et al., 1992). Crucial to meeting this objective was verification that a continuous sedimentary section was recovered at each drill site. Portions of the sedimentary sequence are often missing between two successive APC cores in a single hole. Thus, the only means of meeting the objective of continuous section recovery is by drilling multiple adjacent holes, offset in depth, at each site. A strategy was developed for Leg 138 to verify section recovery in near real time.

Development of a shipboard composite section involved the use of high-resolution, nonintrusively measured, sedimentary parameters (GRAPE, magnetic susceptibility, and digital color reflectance). These parameters were measured in almost every core and could be correlated among adjacent holes at every drilled site. Development of the shipboard composite depth section involved only a translation of cores along a depth scale, as illustrated in Figure 1. Depths measured in meters below the seafloor (mbsf) were transformed to a composite depth scale (mcd, meters composite depth) by adding a constant to the mbsf depth for each core (Mayer, Pisias, Janecek, et al., 1992; Hagelberg et al., 1992).

Although useful for shipboard core correlations, developing a composite depth scale by adding a constant to the original depth scale for every core was of only limited value. The Leg 138 Shipboard Scientific Party agreed that differential stretching or squeezing *within* a 9-m core due to physical disturbance during coring or by natural variations in local sedimentation between adjacent holes would not considered in the shipboard compositing process. However, GRAPE data as well as core photos (Fig. 2) show prevalent nonuniform distortion of sediment within cores. To build continuous records of climate change from deep-sea sediments, it is useful to know the relative level of distortion within a given core as well as among holes, on a scale of centimeters. If the level of depth domain distortion within cores can be quantified, the level of sedimentation rate variability at a single site and the extent to which local differences in sedimentation occur among adjacent holes can be examined.

Post-cruise processing of the GRAPE wet-bulk density records from Leg 138, based on these considerations, led to a revised composite depth scale. This study documents how fine-scale correlation on the order of centimeters was accomplished during post-cruise study. The results are presented in four sections:

1. We introduce the problems that have necessitated composite section development and give a historical review of previous strategies of composite depth formation, concluding with Leg 138 efforts.
2. We present the strategy for post-cruise refinement of the Leg 138 composite depth scales. We demonstrate how the individual GRAPE records in adjacent holes can be "stacked" to produce site-representative bulk density estimates having reduced variance.
3. We develop an error analysis of the amplitudes of GRAPE records for Sites 846 through 852. Error estimates are useful because it is possible to analyze whether within-site as well as between-site differences in GRAPE amplitudes are significant.
4. We investigate the extent of within-site variability in depth-scale distortion. Although some depth-scale distortion in one core relative to another is likely to be induced by the coring process, some is likely to be related to the natural variability of sediment composition in a small geographic area. Characterizing this variability has not been possible

[1] Pisias, N.G., Mayer, L.A., Janecek, T.R., Palmer-Julson, A., and van Andel, T.H. (Eds.), 1995. *Proc. ODP, Sci. Results,* 138: College Station, TX (Ocean Drilling Program).
[2] College of Oceanic and Atmospheric Sciences, Oregon State University, Corvallis, OR, U.S.A.
[3] Now at Graduate School of Oceanography, University of Rhode Island, Narragansett, RI, U.S.A.
[4] University of Cambridge, Godwin Laboratory, Free School Lane, Cambridge CB2 3RS, United Kingdom.

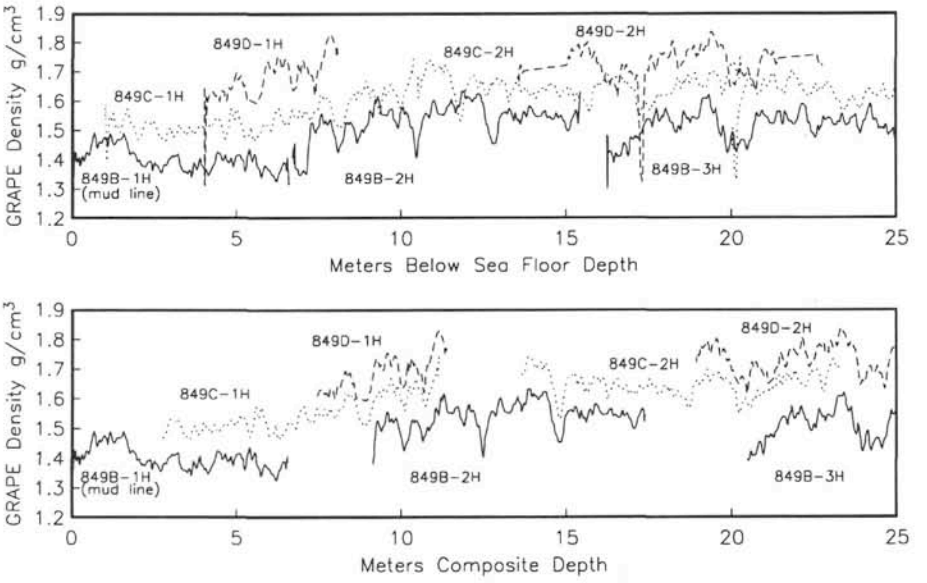


Figure 1. Composite depth section example (GRAPE only) illustrating how cores are moved along a depth scale to arrive at a maximum correlation between adjacent holes. Top: uncleaned but smoothed GRAPE bulk density from the top 25 m of Site 849 on the mbsf (meters below seafloor) depth scale. Bottom: Site 849 GRAPE data after cleaning and on the mcd (meters composite depth) scale. Solid line = Hole 849B; dotted line = Hole 849C; dashed line = Hole 849D. GRAPE density values for Holes 849C and 849D are offset for clarity.

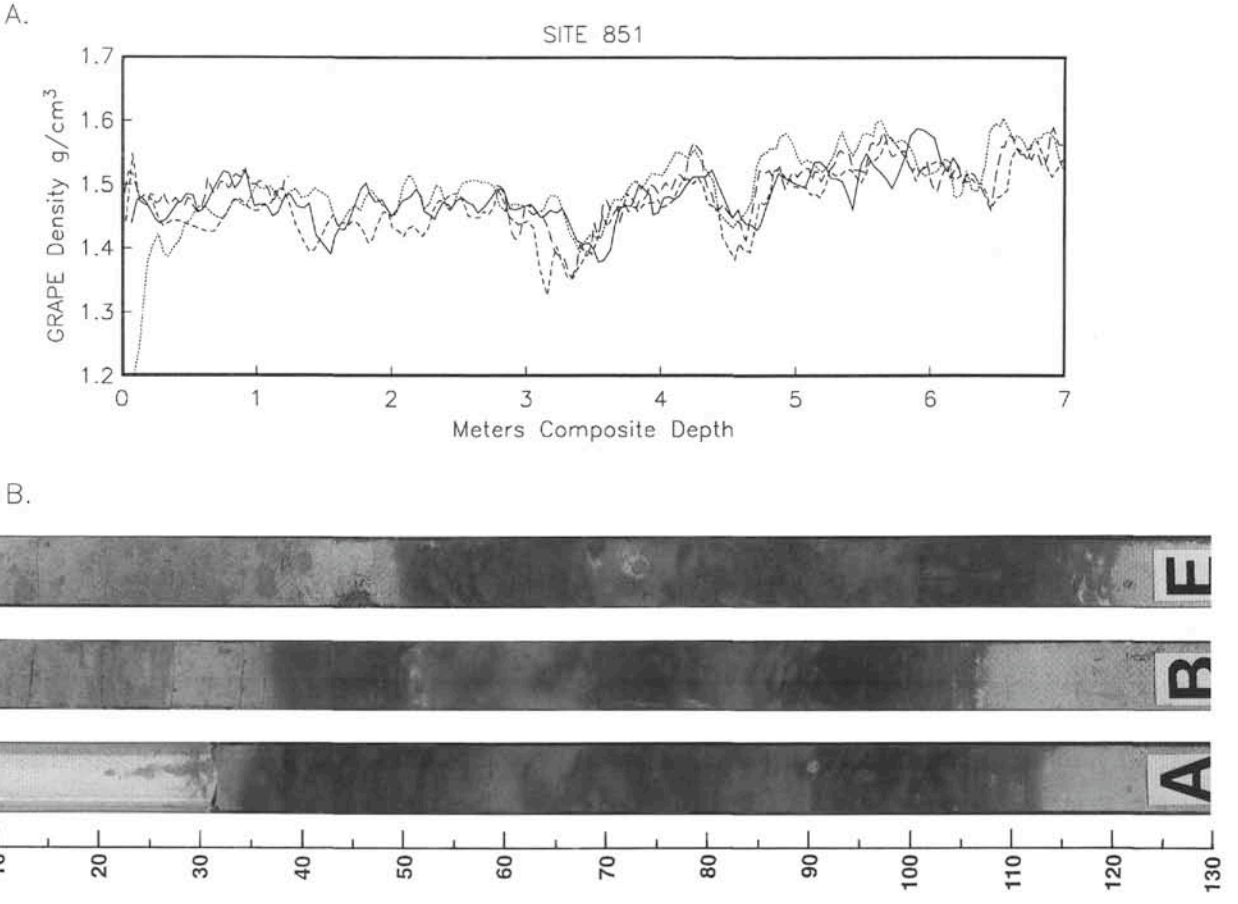


Figure 2. Cores from four adjacent holes in Site 851 indicate coring distortion and local sedimentation variability on a within-core (<9 m) basis. **A.** Site 851 GRAPE records on the shipboard mcd scale from Holes 851A (solid line), 851B (small dash), 851D (medium dash), and 851E (large dash). **B.** Core photos from the same depth interval (1.5–3.5 mcd) also illustrate small-scale depth variability.

previously. Variability in core distortion within a small geographic area has implications for sedimentation rate variability and subsequent development of age models. The level of distortion required to correlate adjacent holes at high-resolution is used to predict the range of sedimentation rate variability, which may be anticipated purely as a result of small-scale variations in sedimentation.

## SCIENTIFIC BACKGROUND

### History of Composite Section Development

In 1979, Deep Sea Drilling Project (DSDP) Leg 68 was dedicated to the use of the hydraulic piston corer (HPC). This leg marked the beginning of recovery of relatively undisturbed sediments suitable for high-resolution paleoceanographic analyses. Leg 68 also marked the beginning of drilling of overlapping holes at one site for documenting the recovery of the complete stratigraphic record at a drill site (Prell et al., 1982). Gardner (1982) and Kent and Spariosu (1982) constructed composite depth sections for multiple drilled Sites 502 and 503, based on carbonate and magnetostratigraphy. By DSDP Leg 69, Shackleton and Hall (1983) observed coring gaps of "several tens of centimeters" between successive 4.5-m HPC cores in Site 504. This observation reinforced the need for multiple drilling of offset holes to obtain continuous paleoceanographic records. Before the advent of the HPC, however, precise stratigraphic correlation of this nature between adjacent holes could not be considered.

The first drilling leg to document explicitly the difficulties encountered when determining a continuous section was DSDP Leg 86 (Heath et al., 1985). Alignment of lithologic and magnetic boundaries demonstrated intervals of double-cored sediments in Holes 576 and 576B and intervals of nonrecovery in Hole 576B. Heath et al. (1985) estimated from this alignment of cores that about 20% of HPC-recovered core might be stratigraphically suspect. Shackleton et al. (1985) noted that biostratigraphic, magnetostratigraphic, and stable isotope events are not observed at the same reported depth (depth below the seafloor) in adjacent holes. These depth discrepancies were addressed by developing a composite depth section. Stable isotope and paleomagnetic stratigraphy were used to adjust sub-bottom depths for each hole at DSDP Site 577.

DSDP Leg 94 marked the beginning of the use of the APC. During this cruise, considerable attention was given to between-hole correlations and total-section recovery (Ruddiman et al., 1987). Color variations, caused primarily by variations in percentages of $CaCO_3$ and documented in core photographs, were the primary correlation tool between adjacent holes at Sites 607 through 611. Ruddiman et al. (1987) documented in detail section continuity and depth offsets between adjacent holes. For the first time, a detailed discussion of factors leading to core recovery and coring gaps was presented. They estimated that gaps on the order of 0.5 to 1 m are present between successive cores in a given hole. During post-cruise scientific study, Ruddiman et al. (1989) and Raymo et al. (1989) used visual core color, percentages of $CaCO_3$, and magnetic data to determine a high-resolution composite section for Sites 607 and 609. Continuous sedimentary sections for Sites 607 and 609 were formed by patching coring gaps from Hole A with sediments from Hole B.

During ODP Leg 108, whole-core magnetic susceptibility and *P*-wave velocity measurements taken at a 5-cm resolution were used in attempts to correlate between offset holes at Sites 659 through 665, and Site 667 (Ruddiman et al., 1988; Bloemendal et al., 1988). This study represented a significant advance in documenting sediment section continuity in that it used rapidly acquired, nonintrusive, high-resolution sedimentary parameters that are routinely collected during ODP legs. However, at several sites (662–665), magnetic susceptibility signals were too low, and *P*-wave velocities unreliable; at these sites, a composite section was determined by correlation of percentages of $CaCO_3$ and visual inspection of core color. As in Leg 94, a continuous sedimentary section was formed by splicing two holes (e.g., Karlin et al., 1989).

An interhole mapping strategy was applied to Site 677 sediments during ODP Leg 111 (Alexandrovich and Hays, 1989). Tephra layers and biostratigraphic datums were used for initial correlations between Holes 677A and 677B. Subsequent analyses of carbonate and opal at 50-cm sampling intervals were used to correlate between the two holes drilled at Site 677 as well as to nearby DSDP Site 504. Inverse correlation was used to define an optimal mapping function between the records. Similar to the earlier study by Ruddiman et al. (1987), gaps of 1 to 2 m were identified between successive cores in each hole. Subsequent higher-resolution correlations with oxygen isotope analyses by Shackleton and Hall (1989) and Shackleton et al. (1990) resulted in a detailed composite section for Site 677. In addition, Shackleton et al. (1990) documented the "growth" of composite section depths downcore. After aligning cores from parallel holes, it was demonstrated that the resulting composite "sample" of the sediment column was approximately 10% longer than the shipboard-measured length of section actually cored.

During ODP Leg 114, a composite depth section was generated for Site 704 by using color boundaries and by correlating high-resolution measurements of carbonate and opal data from the cores (Froelich et al., 1991). These data were compared to borehole log data to confirm intervals of missing and disturbed sediments. In limited intervals of the record, logging data were correlated successfully to coring records, and intervals of high coring disturbance were identified. A discrepancy between the composite section depths and logging depths also was noted.

Whole-core magnetic susceptibility measurements were used in lithostratigraphic correlation during ODP Leg 115 (Robinson, 1990). Magnetic susceptibility measurements were collected at 3- to 10-cm intervals in adjacent holes at Sites 706, 709, 710, and 711 during Leg 115. A composite section was compiled for these sites. As with previous compositing efforts, gaps between successive cores on the order of 1 to 2 m were identified.

During ODP Leg 117, magnetic susceptibility measurements also were valuable for constructing stratigraphically complete records extending back 3.2 m.y. at Sites 721 and 722 (deMenocal et al., 1991; Murray and Prell, 1991). As noted during Leg 111, the complete composite section was 7% to 10% longer than the depth of the section below the seafloor measured by the drill string.

Three adjacent holes were used for developing a composite section for Site 758, ODP Leg 121 (Farrell and Janecek, 1991). As with earlier legs, although APC recovery was 100% to 105%, gaps as large as 2.7 m were revealed between successive cores. Magnetic susceptibility was a primary correlation tool, but the percentage of $CaCO_3$, the coarse fraction, and oxygen isotope records were used to construct a composite section. Attempts were made to resolve depth discrepancies using borehole logs. Although these were not resolved, comparison of logging data with core data was recognized as a means to resolve the discrepancy between ODP-measured core depths and the composite section depths, which are approximately 10% greater.

The consistent outcome of a "stretched" composite section presents several dilemmas. Section recovery is often documented at greater than 100%, meaning that the length of sediment recovered is greater than the advance of the drill string. However, the composite depth section suggests that only approximately 90% of the true sedimentary sequence is recovered in a single hole. In addition, if composite section lengths are 10% greater than drill string lengths, what is the true depth of the recovered sediment?

### Leg 138 Shipboard Correlations

The importance of determining continuity of the sedimentary section, as indicated by the above efforts, suggests that composite section development should be a first-order priority for paleoceanographic drilling studies. Much of the previous effort in composite section development was conducted post-cruise. During ODP Leg 138, verification of a composite section became a part of the drilling

strategy. This produced two significant advances: first, section recovery was monitored in as close to real time as possible, and composite sections were developed at sea, as discussed below. Borehole logs also were incorporated as a means to resolve differences between drill string-measured depths and composite depths. Second, sufficient high-resolution data was collected from multiple holes and sites to consider the impact of small-scale (e.g., local) variability in sedimentation.

The motivation for concentrating efforts during Leg 138 on GRAPE wet-bulk density measurements for interhole and intersite correlations lies in the effectiveness of wet-bulk density as a carbonate proxy in the central and eastern equatorial Pacific Ocean (Mayer, 1980, 1991; Hagelberg et al., this volume). That carbonate records are correlatable over large regions of the Pacific was demonstrated more than 20 yr ago by Hays et al. (1969) and was recently extended to very broad regions using seismic studies (Mayer et al., 1986). During Leg 138, GRAPE and at least two other high-resolution sedimentary parameters, magnetic susceptibility and digital color reflectance (Mix et al., 1992), were used to construct composite depth sections. Advantages of these three sedimentary parameters are (1) that all of them can be collected nonintrusively, (2) they can be measured on every core, and (3) the sampling resolution is 1 to 5 cm. Interactive software was written to examine these data from multiple holes and to develop a composite depth scale while at the drilling site. The sub-bottom depth for each core in each hole at a given site was adjusted to maximize the correlation between holes of each sedimentary parameter simultaneously. These adjustments involved an additive depth constant. In almost all cases, this constant was positive, which resulted in the depth of each core being slightly deeper in the composite section than its shipboard sub-bottom depth indicated. The effect of this adjustment can be seen by comparing the multiple-hole GRAPE data in Figure 1. The modified depth scale defined by these adjustments is referred to as meters composite depth (mcd). The three different sedimentary parameters often displayed distinctly different variations downcore and can be considered as independent checks. Thus, confidence in the interhole correlations was derived from cross-checking among these three parameters (Fig. 3).

The composite depth section formed at each site was at least 10% longer than the mbsf scale (Hagelberg et al., 1992). As in previous ODP legs, although core recovery often exceeded 100%, less than 90% of the sedimentary sequence was recovered in any given hole. While the composite depth sections determined during Leg 138 may not be unique solutions, the shipboard composites considered at least three different sedimentary parameters from all drill holes in all cores at each site. Comparison of the shipboard composite sections to any other composite reconstruction that does not take advantage of the full array of data available at each site may be misleading, as use of a reduced data set will almost surely lead to different between-core offsets. Preliminary shipboard results demonstrated that mbsf depths are closer to logging depths. A simple scaling of the shipboard composite depths to log depths resulted in a good first-order match between logs and core data (e.g., Fig. 4 in Hagelberg et al., 1992). Present work includes the integration of coring data with logging data by mapping composite depths to logging depths (e.g., Harris et al., this volume).

Shipboard composite section results for Sites 844 through 854 were presented in both tabular and graphical forms in the initial shipboard reports. From these data, a single spliced record of GRAPE and other parameters was obtained. These results set the stage for detailed post-cruise studies and for refinement of the composite depth scale to the order of centimeters, as discussed below.

## METHODS

The quality of the high-resolution multiparameter data collected during Leg 138 and the initial composite depth scale for each site make this study possible. Note that from every Leg 138 site, there are multiple measurements of GRAPE wet-bulk density, color, and magnetic susceptibility over much of the drilled section (Fig. 3). In previous paleoceanographic studies making use of composite depth sections from adjacent holes, investigators have "spliced" between adjacent holes to arrive at a single high-resolution record (e.g., Ruddiman et al., 1989, Raymo et al., 1989, Murray and Prell, 1991). Selecting a single hole as a reference, gaps between cores are filled in with data from the adjacent hole or holes. This is often the best approach, as isotopic and geochemical analyses of core data are time consuming, and collecting data from multiple holes often is not possible. With remote measurements, such as GRAPE, however, it is possible to use all data from all holes at the same depth in a given site to arrive at a single estimate. One can consider each adjacent hole as a separate realization of the same sedimentary sequence. A robust estimate of the wet-bulk density that is characteristic of the entire drill site rather than any single hole can be accomplished by averaging the measurements. To do this, however, a composite depth scale on the order of the sampling interval (a few centimeters) is necessary. Thus, a refinement of the shipboard composite depth scale is required. During post-cruise processing of the Leg 138 GRAPE data, such a refinement was accomplished by using inverse correlation.

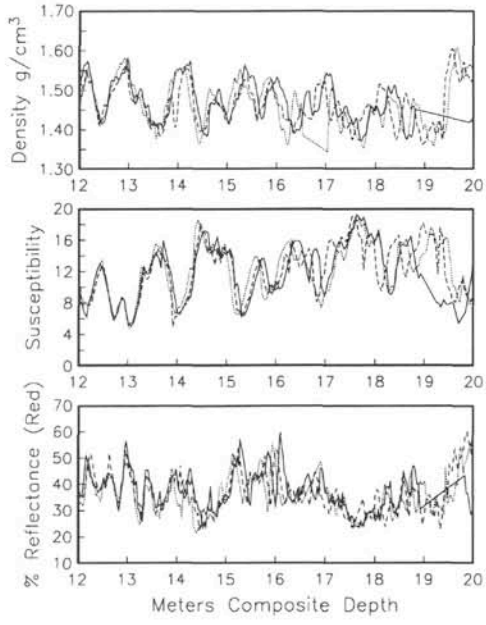


Figure 3. GRAPE, magnetic susceptibility, and color reflectance records from a portion of Site 852 illustrate the presence of multiple measurements over the same depth interval. Solid line = Hole 852B; dotted line = Hole 852C; dashed line = Hole 852D.

Inverse correlation is a means of objectively correlating distorted temporal or spatial signals to an undistorted (reference) signal via some mapping function. The approach developed by Martinson et al. (1982) sought to define a mapping function based on maximum coherence between the two signals and minimal error. This mapping function takes the form of a Fourier sine series. Inverse correlation has been used to correlate data between adjacent holes and nearby drill sites in previous DSDP and ODP studies (Alexandrovich and Hays, 1989; deMenocal et al., 1991). This tool is now of relatively common use in paleoceanographic time series development (e.g., Martinson et al., 1987).

Although magnetic susceptibility and color reflectance data are equally suitable for high-resolution correlation between holes, primary correlations were made using the Leg 138 GRAPE records for several reasons. First, GRAPE data are most easily related to a sedimentary parameter ($CaCO_3$ percentage in a two component carbonate-opal system). Second, the GRAPE data have a relatively high signal-

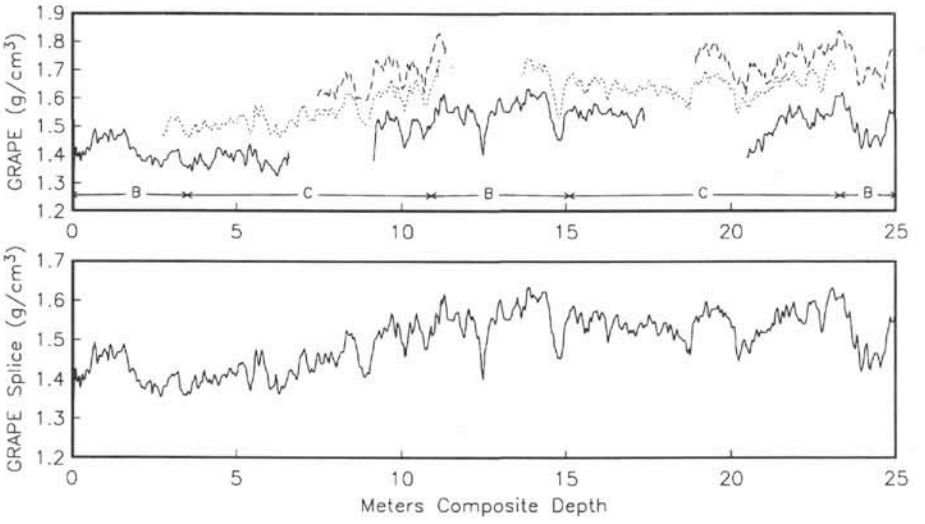


Figure 4. Development of the "shipboard splice" for the top 25 m of Site 849. Top = GRAPE density from three holes from Site 849 on the composite depth scale (solid line = Hole 849B; dotted line = Hole 849C; dashed line = Hole 849D). The letters at the bottom indicate from which hole the shipboard splice was selected for that depth interval. GRAPE values for Holes 849C and 849D are offset for clarity. Bottom = spliced GRAPE record that results from moving between holes, as indicated in top panel.

to-noise ratio at most sites. Third, of the three measured parameters used in composite section development, GRAPE data have the highest sampling resolution. Samples can be collected continuously, with independence of the estimates limited by the width of the gamma-ray beam that passes through the sediment core (approximately 1 cm). Finally, a single "shipboard splice" of GRAPE data had been assembled for each site by N.J. Shackleton after development of the shipboard composite depth section. This spliced record, which used GRAPE data from multiple holes, could be used as a reference signal for the other holes, as discussed below. While the susceptibility and color reflectance data were not used in the inverse mapping step, these data provide a powerful independent check on the correlation defined using the GRAPE data. However, in a few limited intervals where GRAPE wet-bulk density variability was low, susceptibility and color became primary correlation tools.

In limited intervals of each core (primarily at the core tops and bottoms), GRAPE data could not be used for refining the composite section because of anomalously low wet-bulk densities. For the purpose of developing a single composite GRAPE record, this was not a concern as the GRAPE data over these intervals were disregarded. In general, the intervals of core containing anomalously low densities are disturbed and are not of interest. However, for the purposes of developing a high-resolution depth scale for all of the cored section, color reflectance was substituted in these intervals.

GRAPE measurements have significant high-frequency variability, some of which is noise (see discussion below). To improve initial correlation, records were smoothed to a 2-cm resolution using a Gaussian filter. As discussed and illustrated by Martinson et al. (1982), low pass filtering (smoothing) aids recovery of the optimal mapping function by improving the first guess. All of the GRAPE records used in mapping were smoothed beforehand in this manner.

For the Leg 138 drill sites, selection of a reference signal for which to map every core ("distorted" signal) is necessarily somewhat arbitrary, as virtually every overlapping core contains some level of variability as a result of both coring distortion and natural local variability. For each site, the reference signal used was the GRAPE wet-bulk density shipboard splice (Mayer, Pisias, Janecek, et al., 1992). The shipboard splice was chosen subjectively from a qualitative assessment of the amplitude and resolution of the GRAPE records between adjacent holes at each site. During construction of the spliced record, attempts were made to minimize the number of jumps between adjacent holes necessary to arrive at a single record. An example section from Site 849 is given in Figure 4. Shipboard splices of GRAPE wet-bulk density for Sites 844 through 854 are illustrated in the back-pocket figure of the Leg 138 *Initial Reports* volume (Mayer, Pisias, Janecek, et al., 1992). The tie points for each splice are given in Table 1. The shipboard splice made use of all available data from multiple holes at each site, rather than limited data from a few overlapping holes. For this reason, and because the shipboard splice avoided the use of obviously distorted or disturbed sections of core, this record was chosen as the most suitable *relative* composite reference signal for inverse correlation. Although not all core distortion can be addressed in this manner, all of the multiple-hole data can be correlated to a common depth scale. This provides a *relative* measure of core distortion. In a few cases, the section of core chosen as the reference was discovered to be more distorted than the same section in other holes after mapping. Further adjustments relating to distortion of the final stacked record were embedded in time-domain chronology adjustments (Shackleton et al., this volume).

At Sites 846 through 852, individual cores in each hole were mapped, in turn, to the corresponding section of the shipboard splice reference. Note that in some intervals this means that part of a record is mapped to itself. For each core, a mapping function that transforms depth in core in mcd to depth in core rmcd (revised meters composite depth) was produced. The number of coefficients used in the mapping function was chosen iteratively. Beginning with three Fourier coefficients, additional coefficients were added until the coherence between the reference (splice) and the distorted core signal was maximized, or until a further increase in coherence required an unusually large core distortion. Although inverse correlation is in itself an objective approach to signal correlation, the final step of determining the number of Fourier coefficients to be used when determining an optimal mapping function is subjective. We attempted to use the smallest number of Fourier coefficients necessary to obtain maximal coherence without inducing physically unreasonable core distortion. This was accomplished by attempting to minimize large changes in the slope of the mapping function, as suggested by Martinson et al. (1982). The number of coefficients used for mapping each core ranged from 7 to 47. Figure 5 gives examples of two mapping functions from two Site 847 cores, one where 15 coefficients gives very high coherence, and one

**Table 1. The tie points used to construct the shipboard splices of GRAPE data (Mayer, Pisias, Janecek, et al., 1992).**

| Site 844 | | Site 845 | | Site 846 | | Site 847 | | Site 848 | | Site 849 | | Site 850 | | Site 851 | | Site 852 | | Site 853 | | Site 854 | |
|---|---|---|---|---|---|---|---|---|---|---|---|---|---|---|---|---|---|---|---|---|---|
| mcd[a] | Hole | mcd | Hole | mcd | Hole | mcd | Hole | mcd | Hole | mcd | Hole | mcd | Hole | mcd | Hole | mcd | Hole | mcd | Hole | mcd | Hole |
| 0.0 | C | 0.0 | A | 0.0 | B | 0.0 | B | 0.0 | B | 0.0 | B | 0.0 | A | 0.0 | D | 0.0 | A | 0.0 | D | 0.0 | C |
| 4.5 | B | 6.0 | B | 4.0 | C | 5.0 | C | 1.3 | A | 3.5 | C | 6.4 | B | 9.3 | C | 1.1 | D | 7.5 | B | 3.2 | B |
| 14.4 | C | 9.5 | A | 10.5 | B | 8.0 | B | 11.8 | C | 10.9 | B | 10.4 | A | 14.5 | B | 10.4 | B | 13.0 | D | 4.8 | C |
| 18.3 | B | 27.0 | C | 16.0 | D | 14.0 | C | 16.9 | B | 15.1 | C | 17.0 | B | 18.2 | C | 15.0 | D | 20.0 | B | 14.0 | B |
| 21.5 | C | 29.8 | A | 23.0 | B | 21.2 | D | 24.5 | D | 23.3 | B | 20.8 | A | 23.7 | B | 20.5 | B | 29.2 | D | 15.8 | C |
| 29.7 | D | 36.8 | C | 27.6 | D | 24.5 | C | 27.8 | B | 27.2 | C | 28.2 | B | 30.0 | E | 28.6 | C | 31.1 | B | 23.6 | B |
| 38.2 | B | 40.4 | A | 32.0 | B | 32.2 | D | 35.0 | D | 34.4 | B | 32.3 | A | 32.3 | B | 35.7 | D | 32.6 | D | 39.3 | C |
| 43.2 | C | 49.0 | B | 35.0 | C | 38.0 | B | 36.5 | B | 38.9 | C | 38.0 | B | 41.2 | C | 42.0 | C | 41.8 | B | 41.8 | B |
| 52.0 | B | 50.5 | A | 42.2 | D | 42.3 | D | 43.0 | C | 42.7 | B | 45.0 | A | 47.0 | E | 47.0 | D | 52.3 | B | | |
| 55.7 | C | 58.8 | B | 45.7 | C | 46.0 | C | 47.2 | B | 49.2 | C | 48.2 | B | 54.0 | B | 52.0 | B | 60.6 | D | | |
| 62.5 | B | 60.9 | A | 53.0 | D | 52.0 | D | 53.3 | C | 54.5 | B | 54.0 | A | 61.8 | C | 60.2 | C | 62.7 | B | | |
| 65.8 | C | 69.2 | B | 56.5 | B | 55.5 | C | 57.4 | B | 60.4 | C | 61.0 | B | 66.8 | B | 67.8 | D | 71.0 | D | | |
| 70.9 | B | 72.2 | A | 58.5 | C | 64.4 | D | 64.5 | C | 64.1 | B | 65.0 | A | 72.8 | C | 74.5 | B | | | | |
| 76.6 | C | 79.5 | A | 64.3 | B | 69.0 | C | 69.5 | B | 72.0 | C | 71.9 | B | 75.7 | B | 81.5 | C | | | | |
| 83.8 | B | 82.5 | A | 67.7 | D | 75.8 | D | 76.0 | C | 75.8 | D | 74.5 | A | 83.2 | C | 90.1 | D | | | | |
| 86.9 | C | 90.6 | B | 76.5 | B | 81.0 | C | 81.0 | B | 79.8 | C | 80.4 | B | 86.4 | B | 95.2 | B | | | | |
| 93.6 | B | 95.2 | A | 80.0 | D | 84.4 | D | 87.5 | C | 84.5 | D | | | 92.4 | C | 103.8 | D | | | | |
| 96.3 | C | 101.3 | B | 85.0 | B | 90.5 | C | 92.0 | B | 88.7 | B | | | 99.6 | B | 106.7 | B | | | | |
| 104.0 | B | 108.0 | A | 89.0 | D | 96.5 | B | 98.0 | C | 92.3 | C | | | 103.8 | C | 114.2 | C | | | | |
| 110.5 | C | 111.3 | B | 95.5 | C | 100.0 | C | 101.7 | B | 98.6 | B | | | 108.5 | B | 121.3 | D | | | | |
| 115.0 | B | 115.1 | A | 98.3 | B | 107.0 | D | | | 103.7 | C | | | 115.3 | C | | | | | | |
| 121.4 | C | 117.1 | B | 99.0 | D | 114.0 | C | | | 110.1 | B | | | 121.6 | B | | | | | | |
| 125.0 | B | 119.2 | A | 107.3 | C | 116.5 | D | | | 114.0 | C | | | 126.8 | C | | | | | | |
| 126.9 | C | 123.0 | B | 111.0 | D | 122.2 | C | | | 116.5 | D | | | 132.3 | B | | | | | | |
| 133.9 | B | 127.5 | A | 117.0 | C | 126.5 | D | | | 123.4 | B | | | 137.5 | C | | | | | | |
| 138.3 | C | 134.2 | B | 120.3 | D | 134.5 | C | | | 125.5 | D | | | 142.4 | B | | | | | | |
| 146.3 | B | 136.4 | A | 128.0 | C | 138.5 | D | | | 128.8 | B | | | 147.1 | C | | | | | | |
| 148.5 | C | 145.0 | B | 130.5 | D | 143.8 | C | | | 137.0 | D | | | 149.9 | B | | | | | | |
| 157.0 | B | 151.0 | A | 140.0 | C | 147.8 | B | | | 151.5 | B | | | 168.5 | E | | | | | | |
| 159.4 | C | 156.4 | B | 142.4 | D | 155.0 | C | | | 157.7 | D | | | 174.0 | B | | | | | | |
| 167.1 | B | 159.3 | A | 145.8 | C | 159.2 | B | | | 163.0 | B | | | 182.6 | E | | | | | | |
| 170.7 | C | 167.0 | B | 152.2 | B | 202.3 | C | | | 167.5 | D | | | 188.3 | B | | | | | | |
| 176.2 | B | 174.5 | A | 155.0 | D | 204.8 | B | | | 175.0 | B | | | 194.5 | E | | | | | | |
| 179.1 | C | 178.1 | B | 160.0 | C | | | | | 180.5 | D | | | 203.5 | B | | | | | | |
| 184.3 | B | 182.8 | A | 163.0 | B | | | | | 186.2 | B | | | 208.3 | E | | | | | | |
| 190.6 | C | 188.3 | B | 165.0 | D | | | | | 192.6 | D | | | 217.0 | B | | | | | | |
| 197.6 | B | 192.0 | A | 173.0 | B | | | | | 198.5 | B | | | 224.5 | E | | | | | | |
| | | 197.7 | B | 176.5 | D | | | | | 202.5 | D | | | 230.8 | B | | | | | | |
| | | 203.2 | A | 180.2 | C | | | | | 208.9 | B | | | 236.2 | E | | | | | | |
| | | 210.3 | B | 185.2 | B | | | | | 215.0 | D | | | 238.0 | B | | | | | | |
| | | 214.0 | A | 188.5 | C | | | | | 220.5 | B | | | 245.0 | E | | | | | | |
| | | 218.7 | B | 194.3 | B | | | | | 225.5 | D | | | 252.4 | B | | | | | | |
| | | 233.5 | A | 200.0 | C | | | | | 231.0 | B | | | 261.1 | E | | | | | | |
| | | | | 206.5 | B | | | | | 236.8 | D | | | 264.0 | B | | | | | | |
| | | | | 209.7 | D | | | | | 243.4 | B | | | 272.0 | E | | | | | | |
| | | | | 215.3 | B | | | | | 245.4 | D | | | 277.8 | B | | | | | | |
| | | | | 224.2 | D | | | | | 252.9 | B | | | 284.5 | E | | | | | | |
| | | | | 228.0 | B | | | | | 257.8 | D | | | 293.3 | B | | | | | | |
| | | | | 236.5 | D | | | | | 263.5 | B | | | 296.2 | E | | | | | | |
| | | | | 240.7 | B | | | | | 268.0 | D | | | 301.0 | B | | | | | | |
| | | | | 248.0 | D | | | | | 270.9 | B | | | 309.8 | E | | | | | | |
| | | | | 252.0 | B | | | | | 286.7 | D | | | 316.3 | B | | | | | | |
| | | | | 260.8 | D | | | | | 293.6 | B | | | 320.6 | E | | | | | | |
| | | | | 261.5 | B | | | | | 297.2 | D | | | 329.0 | B | | | | | | |
| | | | | | | | | | | 304.2 | B | | | 339.4 | E | | | | | | |
| | | | | | | | | | | 307.2 | D | | | 340.5 | B | | | | | | |
| | | | | | | | | | | 315.5 | B | | | 350.7 | E | | | | | | |
| | | | | | | | | | | 317.8 | D | | | 358.7 | B | | | | | | |
| | | | | | | | | | | 326.3 | B | | | 362.0 | E | | | | | | |
| | | | | | | | | | | 329.1 | D | | | 368.5 | B | | | | | | |
| | | | | | | | | | | 336.8 | B | | | 373.0 | E | | | | | | |
| | | | | | | | | | | 338.9 | D | | | 380.3 | B | | | | | | |
| | | | | | | | | | | 345.8 | B | | | | | | | | | | |
| | | | | | | | | | | 350.3 | D | | | | | | | | | | |
| | | | | | | | | | | 357.8 | B | | | | | | | | | | |
| | | | | | | | | | | 361.0 | D | | | | | | | | | | |
| | | | | | | | | | | 367.9 | B | | | | | | | | | | |

[a]mcd indicates meters composite depth, as described in Mayer, Pisias, Janecek, et al. (1992).

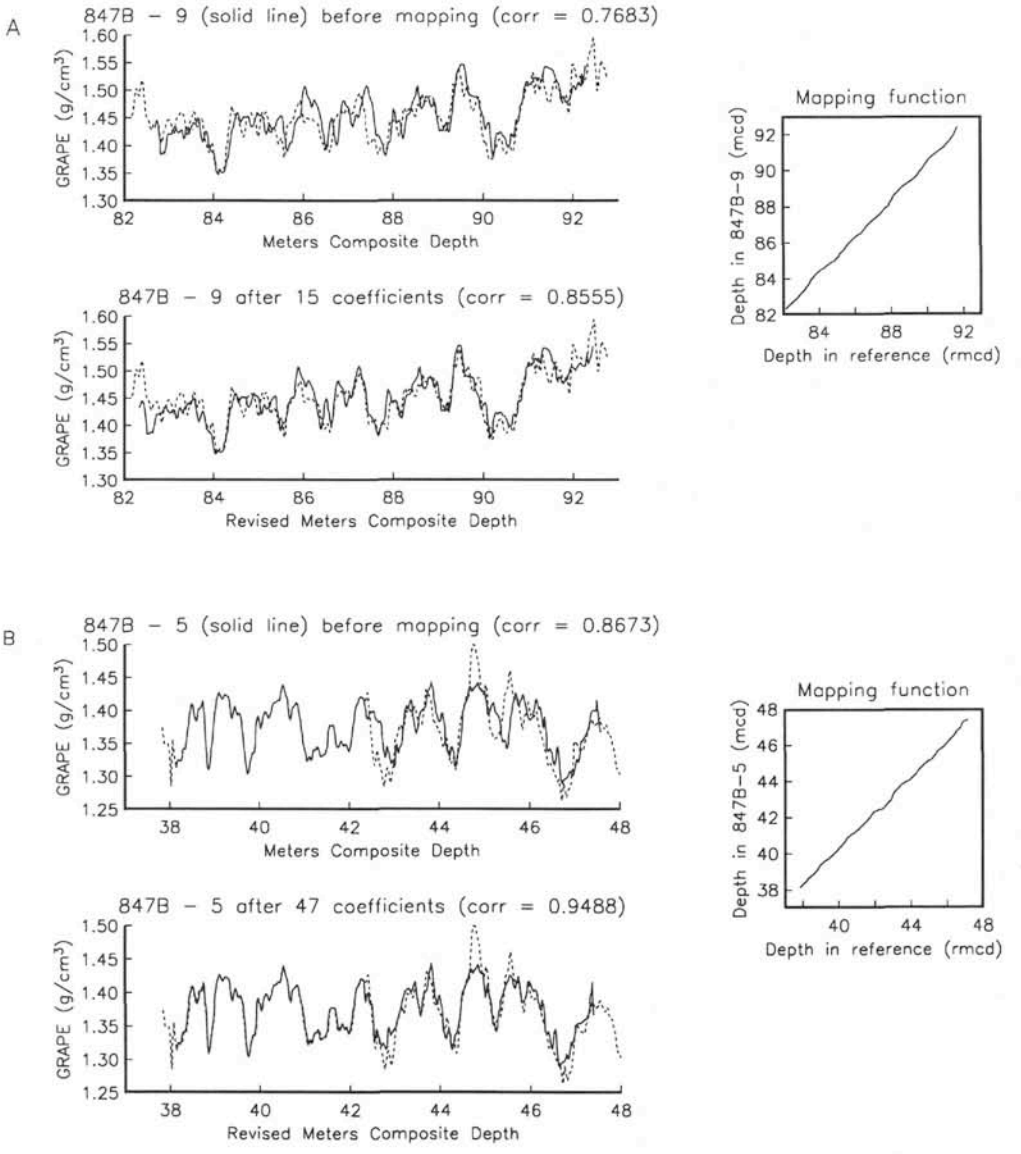


Figure 5. Examples of before (above) and after (below) inverse correlation from two cores at Site 847. The mapping function between depth in core (mcd) and depth in the shipboard splice (rmcd) is shown at right. **A.** Fifteen Fourier coefficients used. **B.** Forty-seven Fourier coefficients used in inverse correlation.

where 47 coefficients were used. In both examples, the correlation between the initial unmapped core interval and the corresponding interval of the shipboard splice increases noticeably without introducing large slope changes into the mapping function.

## RESULTS

Sediments from approximately the past 5 m.y. from Sites 846 through 852 were multiple-APC-cored during Leg 138. Beyond this point, multiple holes are not available at every site for high-resolution correlation. For each of 241 cores from multiple holes, a mapping function was calculated using the technique of Martinson et al. (1982). The mapping function was calculated to maximize the correlation between each individual core and the reference GRAPE record. Table 2 gives the correlation of each core to the reference splice before and after mapping. On average, correlations improved from 0.755 (±0.16) to 0.923 (±0.07). The mapping function defined by the inverse mapping technique allows for each depth within a core to be mapped uniquely into the GRAPE reference record. This transformation changes the depth of any sample in mcd (exclusive of those samples that are a part of the reference) to a new depth scale, rmcd. The transformed depths for Sites 846 through 852 are available on CD-ROM as Appendix (back pocket, this volume).

To check that the mapping functions defined in the GRAPE data are consistent with the other high-resolution data available for the Leg 138 sites, the mapping functions were applied to the corresponding downcore records of magnetic susceptibility and color. The example given in Figure 6 demonstrates that the improvement in correlation between GRAPE data from three holes at Site 852 is also seen in susceptibility and color records. Thus, the susceptibility and color reflectance records do provide a means of confirming correlations based on GRAPE values. Additional confirmation of the mcd and rmcd mapping comes from isotopic time series developed using the compositing scheme (e.g., Mix et al., this volume). Checks of the GRAPE-defined mapping functions with susceptibility and color reflectance data revealed that, in some cases, revision was required to

**Table 2. Correlation of each core to the shipboard splice reference before and after mapping with inverse correlation.**

| Core | Hole 846A | | Hole 846B | | Hole 846C | | Hole 846D | |
|---|---|---|---|---|---|---|---|---|
| 1 | 0.5764 | 0.7051 (31)[a] | 0.7534 | 0.8853 (47) | 0.8549 | 0.9715 (31) | 0.8122 | 0.8729 (15) |
| 2 | | | 0.9282 | 0.9669 (31) | 0.7682 | 0.8799 (31) | 0.8662 | 0.9778 (7) |
| 3 | | | 0.6552 | 0.9276 (31) | 0.7948 | 0.8612 (23) | 0.8270 | 0.9370 (31) |
| 4 | | | 0.7281 | 0.9256 (23) | 0.9544 | 0.9619 (15) | 0.5427 | 0.8626 (23) |
| 5 | | | 0.6302 | 0.8100 (15) | 0.7644 | 0.9628 (31) | 0.5798 | 0.9229 (23) |
| 6 | | | 1.000 | | 0.7244 | 0.9306 (31) | 0.5394 | 0.8723 (31) |
| 7 | | | 0.6645 | 0.8568 (15) | 0.6939 | 0.9120 (39) | 0.7319 | 0.9870 (7) |
| 8 | | | 0.7270 | 0.8678 (7) | 0.7707 | 0.9137 (15) | 0.8068 | 0.9695 (39) |
| 9 | | | 0.8967 | 0.9383 (15) | 0.8947 | 0.9518 (31) | 0.8150 | 0.8555 (7) |
| 10 | | | 0.7129 | 0.9518 (31) | 0.9282 | 0.9639 (31) | 0.9743 | 0.9811 (15) |
| 11 | | | 0.8163 | 0.9238 (19) | 0.6985 | 0.9037 (31) | 0.7977 | 0.9604 (23) |
| 12 | | | 0.6802 | 0.8333 (11) | 0.6750 | 0.8803 (23) | 0.5652 | 0.9710 (23) |
| 13 | | | 0.8204 | 0.9334 (23) | 0.8257 | 0.9606 (31) | 0.9922 | 0.9948 (7) |
| 14 | | | 0.4701 | 0.6377 (15) | 0.6398 | 0.8933 (31) | 0.6538 | 0.8309 (7) |
| 15 | | | 0.9312 | 0.9764 (17) | 0.9091 | 0.9870 (31) | 0.9222 | 0.9880 (23) |
| 16 | | | 0.4237 | 0.9006 (27) | 0.8849 | 0.9613 (31) | 0.8771 | 0.9954 (47) |
| 17 | | | 0.8812 | 0.9508 (31) | 0.9041 | 0.9537 (23) | 0.4440 | 0.9604 (39) |
| 18 | | | 0.7718 | 0.9702 (23) | 0.6685 | 0.9620 (23) | 0.7410 | 0.8892 (15) |
| 19 | | | 0.6416 | 0.9184 (19) | 0.9215 | 0.9773 (31) | 0.3057 | 0.8218 (39) |
| 20 | | | 0.5732 | 0.8883 (31) | 0.5129 | 0.8970 (31) | 0.4713 | 0.9245 (31) |
| 21 | | | 0.6717 | 0.9056 (7) | | | 0.1325 | 0.7281 (23) |
| 22 | | | 0.9166 | 0.9602 (15) | | | 0.6465 | 0.8631 (15) |
| 23 | | | 0.5778 | 0.8601 (23) | | | 0.4808 | 0.8941 (23) |
| 24 | | | 0.9808 | 0.9831 (7) | | | 0.4484 | 0.5360 (7) |
| 25 | | | 0.9755 | | | | 0.4412 | 0.7088 (7) |
| 26 | | | 1.000 | | | | | |

| Core | Hole 847A | | Hole 847B | | Hole 847C | | Hole 847D | |
|---|---|---|---|---|---|---|---|---|
| 1 | 0.8924 | 0.9293 (15) | 0.9118 | 0.9798 (23) | 0.8957 | 0.9554 (23) | (NO GRAPE) | |
| 2 | | | 0.9345 | 0.9823 (23) | 0.8480 | 0.9920 (47) | 0.8970 | 0.9367 (31) |
| 3 | | | 0.8618 | 0.8920 (7) | 0.8594 | 0.9647 (31) | 0.8037 | 0.8989 (15) |
| 4 | | | 0.8123 | 0.9016 (39) | 0.5532 | 0.8092 (31) | 0.8425 | 0.9538 (31) |
| 5 | | | 0.8673 | 0.9488 (47) | 0.7564 | 0.9703 (50) | 0.6685 | 0.8903 (31) |
| 6 | | | 0.7869 | 0.8839 (15) | 0.8093 | 0.9922 (47) | 0.8220 | 0.9309 (15) |
| 7 | | | 0.8061 | 0.9168 (23) | 0.8590 | 0.9750 (31) | 0.6648 | 0.9653 (47) |
| 8 | | | 0.5455 | 0.8473 (31) | 0.6277 | 0.8925 (23) | 0.7164 | 0.9360 (23) |
| 9 | | | 0.7683 | 0.8555 (15) | 0.9199 | 0.9749 (47) | 0.8090 | 0.9577 (15) |
| 10 | | | 0.4147 | 0.8533 (23) | 0.4300 | 0.8828 (31) | 0.6148 | 0.7896 (15) |
| 11 | | | 0.8325 | 0.9258 (23) | 0.4848 | 0.9393 (47) | 0.7911 | 0.9728 (47) |
| 12 | | | 0.8280 | 0.9113 (31) | 0.6573 | 0.9587 (23) | 0.4670 | 0.9712 (39) |
| 13 | | | 0.9569 | 0.9746 (23) | 0.8460 | 0.9033 (23) | 0.8790 | 0.9881 (15) |
| 14 | | | 0.8854 | 0.9595 (15) | 0.6467 | 0.8485 (15) | 0.9312 | 0.9814 (39) |

| Core | Hole 848A | | Hole 848B | | Hole 848C | | Hole 848D | |
|---|---|---|---|---|---|---|---|---|
| 1 | 0.7562 | 0.9846 (39) | 0.8548 | 0.9564 (23) | 0.7430 | 0.8103 (7) | 0.8478 | 0.9206 (15) |
| 2 | | | 0.5216 | 0.9463 (31) | 0.7541 | 0.9667 (31) | 0.6290 | 0.9096 (23) |
| 3 | | | 0.5773 | 0.9718 (39) | 0.8238 | 0.8923 (31) | 0.6450 | 0.9046 (23) |
| 4 | | | 0.9037 | 0.9777 (47) | 0.8316 | 0.9328 (31) | 0.6459 | 0.9262 (23) |
| 5 | | | 0.7216 | 0.9879 (39) | 0.6581 | 0.8220 (23) | 0.4243 | 0.7573 (15) |

| Core | Hole 849A | | Hole 849B | | Hole 849C | | Hole 849D | |
|---|---|---|---|---|---|---|---|---|
| 1 | (No GRAPE) | | 0.7700 | 0.9205 (47) | 0.8676 | 0.9938 (23) | 0.9218 | 0.9613 (15) |
| 2 | | | 0.7765 | 0.9656 (47) | 0.9895 | 0.9944 (47) | 0.7525 | 0.8446 (15) |
| 3 | | | 0.7600 | 0.9042 (31) | 0.8512 | 0.9572 (39) | 0.7125 | 0.8724 (23) |
| 4 | | | 0.6061 | 0.8785 (31) | 0.5232 | 0.9511 (47) | 0.6829 | 0.8901 (31) |
| 5 | | | 0.6202 | 0.9660 (47) | 0.8337 | 0.9557 (31) | 0.8611 | 0.9256 (23) |
| 6 | | | 0.9424 | 0.9880 (47) | 0.9009 | 0.9757 (39) | 0.8399 | 0.8862 (31) |
| 7 | | | 0.7434 | 0.9769 (47) | 0.7224 | 0.9253 (23) | 0.8459 | 0.9593 (47) |
| 8 | | | 0.7256 | 0.9534 (23) | 0.8125 | 0.9770 (31) | 0.6761 | 0.9557 (31) |
| 9 | | | 0.9179 | 0.9704 (7) | 0.9008 | 0.9799 (31) | 0.7519 | 0.9184 (15) |
| 10 | | | 0.9175 | 0.9347 (31) | 0.6598 | 0.9769 (47) | 0.3183 | 0.9258 (23) |
| 11 | | | 0.7714 | 0.9594 (15) | 0.6055 | 0.7614 (31) | 0.8698 | 0.9911 (47) |

| Core | Hole 850A | | Hole 850B | |
|---|---|---|---|---|
| 1 | 0.9413 | 0.9874 (23) | 0.8161 | 0.9568 (23) |
| 2 | 0.7944 | 0.9450 (15) | 0.7921 | 0.9488 (23) |
| 3 | 0.4900 | 0.9265 (23) | 0.4998 | 0.9254 (39) |
| 4 | 0.8221 | 0.9639 (47) | 0.8323 | 0.9794 (47) |
| 5 | 0.6778 | 0.8252 (23) | 0.6805 | 0.9350 (47) |
| 6 | 0.9221 | 0.9796 (15) | 0.9371 | 0.9734 (31) |
| 7 | 0.8091 | 0.9864 (47) | 0.8375 | 0.9301 (47) |
| 8 | 0.7650 | 0.9756 (47) | 0.8269 | 0.9797 (47) |

| Core | Hole 851A | | Hole 851B | | Hole 851C | | Hole 851E | |
|---|---|---|---|---|---|---|---|---|
| 1 | 0.2952 | 0.6123 (7) | 0.6818 | 0.8195 (15) | 0.3567 | 0.7742 (23) | 0.7149 | 0.8427 (23) |
| 2 | | | 0.8810 | 0.9179 (7) | 0.7551 | 0.9259 (23) | 0.4377 | 0.8254 (23) |
| 3 | | | 0.6882 | 0.9265 (39) | 0.5827 | 0.8833 (31) | 0.4944 | 0.9132 (47) |
| 4 | | | 0.8773 | 0.9975 (7) | 0.7679 | 0.9305 (39) | 0.7881 | 0.8746 (15) |
| 5 | | | 0.6331 | 0.8389 (23) | 0.7670 | 0.8786 (39) | 0.8085 | 0.9566 (31) |
| 6 | | | 0.7452 | 0.9720 (23) | 0.7097 | 0.9558 (47) | 0.8394 | 0.9215 (23) |
| 7 | | | 0.8328 | 0.9813 (47) | 0.8196 | 0.9394 (15) | 0.8017 | 0.9273 (31) |
| 8 | | | 0.8476 | 0.9741 (23) | 0.6362 | 0.9097 (23) | 0.7112 | 0.9277 (39) |

| Core | Hole 851D | |
|---|---|---|
| 1 | 0.9500 | 0.9590 (31) |
| 2 | 0.3526 | 0.8202 (23) |

**Table 2 (continued).**

| Core | Hole 852A | | Hole 852B | | Hole 852C | | Hole 852D | |
|---|---|---|---|---|---|---|---|---|
| 1 | 0.9055 | 0.9647 (39) | 0.7469 | 0.9578 (47) | 0.6007 | 0.8671 (15) | 0.9848 | 0.9945 (47) |
| 2 | | | 0.5145 | 0.9712 (15) | 0.8312 | 0.9409 (23) | 0.8827 | 0.9019 (15) |
| 3 | | | 0.8087 | 0.9909 (31) | 0.8734 | 0.9314 (23) | 0.8760 | 0.9672 (47) |
| 4 | | | 0.8415 | 0.9618 (47) | 0.9703 | 0.9752 (23) | 0.9618 | 0.9779 (31) |
| 5 | | | 0.8324 | 0.9453 (39) | 0.9659 | 0.9859 (49) | 0.9618 | 0.9779 (31) |
| 6 | | | 0.8066 | 0.9914 (15) | 0.8087 | 0.9439 (47) | 0.8286 | 0.9186 (15) |
| 7 | | | 0.8205 | 0.9387 (31) | 0.8253 | 0.9937 (47) | 0.9312 | 0.9902 (47) |
| 8 | | | 0.9079 | 0.9659 (31) | 0.8132 | 0.8975 (23) | 0.7660 | 0.8927 (23) |
| 9 | | | 0.8257 | 0.8819 (31) | 0.9943 | 0.9944 (7) | 0.9164 | 0.9670 (47) |
| 10 | | | 0.9209 | 0.9902 (39) | 0.7532 | 0.8672 (31) | 0.9219 | 0.9440 (31) |
| 11 | | | 0.9589 | 0.9780 (23) | 0.4822 | 0.6413 (23) | 0.9279 | 0.9664 (23) |
| 12 | | | 0.6103 | 0.9329 (23) | 0.9851 | 0.9893 (15) | 0.8678 | 0.9644 (23) |

[a]The number in parentheses is the number of coefficents used in the mapping function.

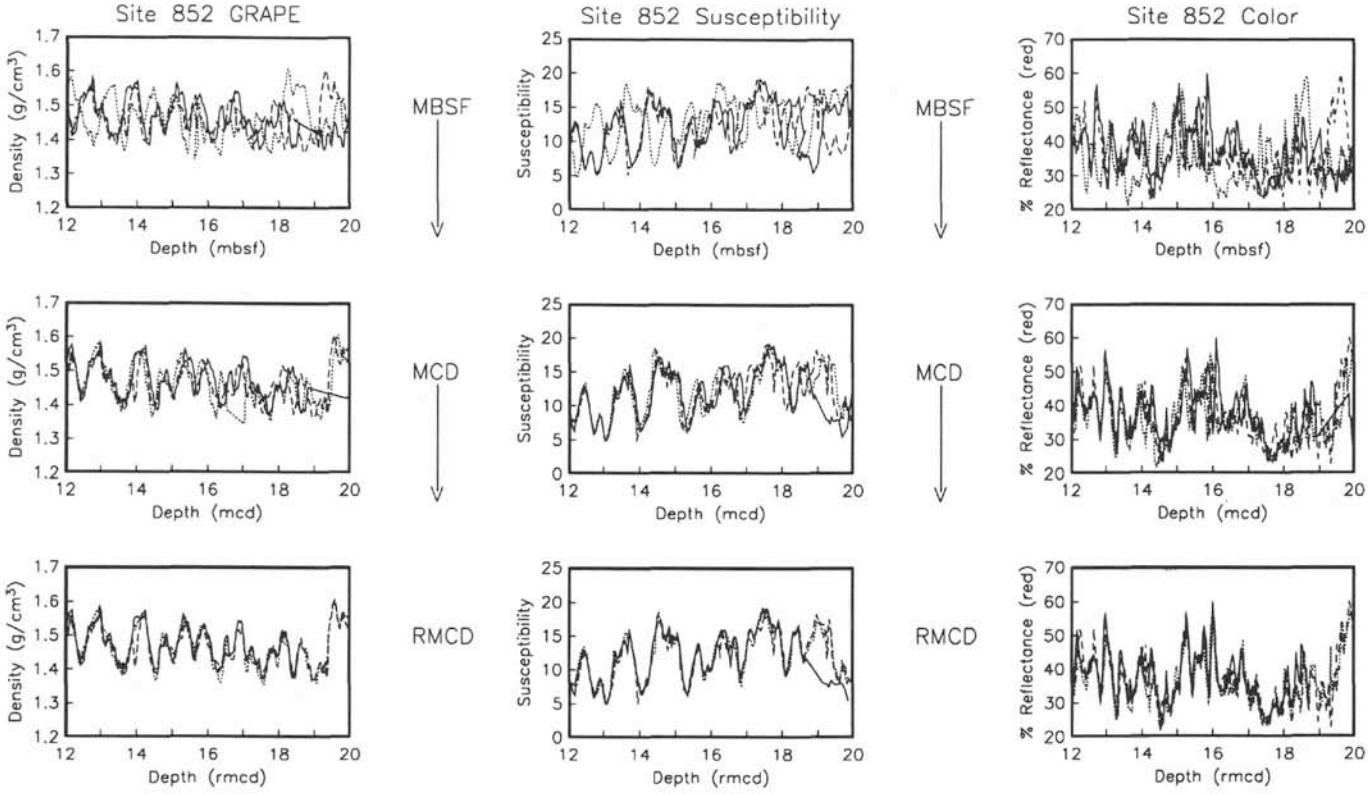


Figure 6. GRAPE, magnetic susceptibility, and color reflectance data from three cores in a portion of Site 852. Top = records from adjacent holes on the mbsf scale. Middle = same records on the mcd scale. Bottom = same records after inverse correlation on the revised meters composite depth (rmcd) scale.

reconcile all three data sets. As these intervals were usually short in duration (often less than 1 m), manual adjustments proved better than inverse correlation.

After mapping all of the multiple-hole GRAPE data to a common depth scale (rmcd), the data from each hole were combined and averaged to form a single depth series of "stacked" GRAPE. Raw data were binned into 2-cm intervals and averaged ("raw" data refers to unsmoothed GRAPE data where only multiple measurements in the same core at the same depths had been binned and averaged). Binning of the raw data adds a sharp jittery character to the resulting record that is unrealistic, as it is an artifact of the binning and is not representative of any of the individual hole records. To reduce this effect, the binned and averaged data were smoothed using a 6-cm Gaussian window in the depth domain. The smoothed stacked GRAPE records for Sites 846 through 852 are shown in Figure 7.

One can consider each record of GRAPE bulk density from each hole at a given site as a separate realization having uncorrelated errors. Averaging the multiple measurements from the adjacent holes decreases the level of noise in the estimates. The number of measurements in each 2 cm bin is not uniformly distributed in depth (nor in time). For each of the Sites 846 through 852 GRAPE stacks, the average number of measurements in each 2-cm bin that is combined to increase the signal/noise level is given in Table 3.

## DISCUSSION

### Error Estimation

Because the inverse correlation provides multiple estimates of GRAPE bulk density at each depth, the sampling error can be quantified. First, however, what is the source of measurement error in the amplitudes of GRAPE wet-bulk density estimates? Boyce (1976) gave a review of the errors encountered when estimating bulk density from GRAPE values. A small error (a maximum of 2%) in wet-bulk density determination occurs if the grain density of the lithology under examination is not known accurately. Also, error can result from random gamma-ray emissions, which have been determined to be on the order of 2% (Boyce, 1976). This error is reduced during shipboard processing of GRAPE data, where some multiple measure-

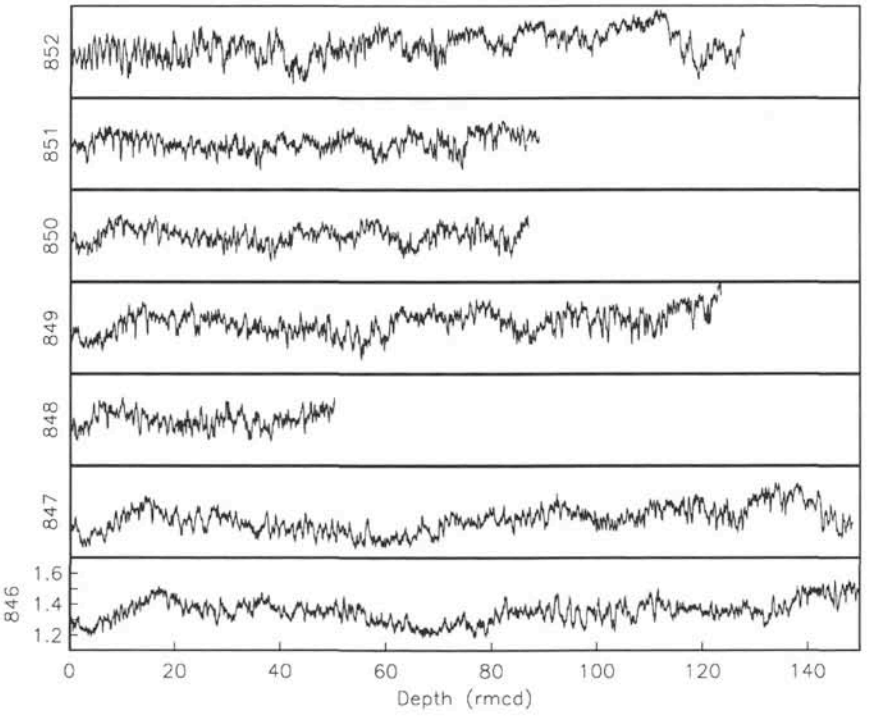


Figure 7. Stacked GRAPE records from Sites 846 to 852 after binning, averaging, and smoothing individual hole records that have been correlated using the shipboard splice through inverse correlation.

**Table 3. Average number of measurements in each 2-cm bin for Sites 846 through 852.**

| Site | Depth range (mcd) | Average number of measurements |
|---|---|---|
| 846 | 0–287 | 1.90 |
| 847 | 0–148 | 2.47 |
| 848 | 0–50 | 2.61 |
| 849 | 0–123 | 2.25 |
| 850 | 0–87 | 1.60 |
| 851 | 0–89 | 1.42 |
| 852 | 0–128 | 2.87 |

ments are taken at exactly the same depth (while the multisensor track pauses to take magnetic susceptibility and *P*-wave velocity measurements) and are averaged. Should the cored material not completely fill the core liner, the gamma ray passing through the core passes through air, water, or slurry, lowering the resulting bulk density measurement. In addition, the gamma-ray beam does not in this case pass through the center of the core. These possible sources of error as well as variation in the thickness of the core liner can influence GRAPE wet-bulk density estimates.

There are a number of ways to estimate sampling errors on the resulting interpolated GRAPE estimates. For example, one might consider the errors as a residual deviation of the raw data values from the resulting smoothed estimates. This involves a comparison of raw data with filtered data that is derived from the raw data. On the other hand, one might consider the errors as simply the standard deviation of the data within any one 2-cm bin, independent of the surrounding data. In practice, the differences between the two methods are not significant. The latter method was chosen because it is more directly tied to the scatter of the raw data within any 2-cm interval. In addition, calculating the standard deviation of the binned data disregards the filtering effects of the Gaussian smoother. Figure 8 shows one standard deviation errors for representative portions of Sites 846 through 852.

There are two significant advantages to having error estimates. First, similar features between the amplitude of GRAPE (carbonate) events at different sites can be compared quantitatively. A primary paleoceanographic objective for use of the GRAPE data is to study spatial changes in carbonate concentration with respect to latitude and longitude in the eastern equatorial Pacific (e.g., Hagelberg et al., this volume). With error estimates, it is possible to quantify whether individual events between sites record significant changes in GRAPE (carbonate), or if site-to-site differences are on the same order as the error at any one site. The second advantage is that one can determine if adjacent features (GRAPE highs and lows) within a given site are significantly different from one another. Error estimates such as this have not been available previously for this kind of geologic data. Both of these advantages are illustrated in the following example.

Shackleton and Shipboard Scientific Party (1992) combined biostratigraphic and magnetostratigraphic events with GRAPE wet-bulk density features from the shipboard splices for Sites 846 through 852 to develop an internally consistent chronostratigraphic framework. A series of GRAPE "events" were identified on the basis of their relation to biostratigraphy and magnetostratigraphy and were correlated to other sites using the GRAPE record. An example event, Event F, was identified as a sharp density maximum that occurs below the Gilbert/Gauss magnetic boundary and near two nannofossil biostratigraphic events, the extinction of *Reticulofenestra pseudoumbilicus* and the upper limit of *Spenolithus abies* (Shackleton and Shipboard Scientific Party, 1992). The age of this event is approximately 3.44 Ma. The depth of this event at each site (as determined in the shipboard splice) is given in Table 4 (since depths are given from the shipboard splice reference, mcd = rmcd). Figure 9 shows the GRAPE density from these depth intervals in the stacked records, with one standard deviation errors. Qualitatively, the peaks at Sites 846 and 847 are fairly large relative to the peaks at Sites 848 and 850. As error estimates of the density records have been developed, the significance of these differences can be accomplished through an analysis of variance.

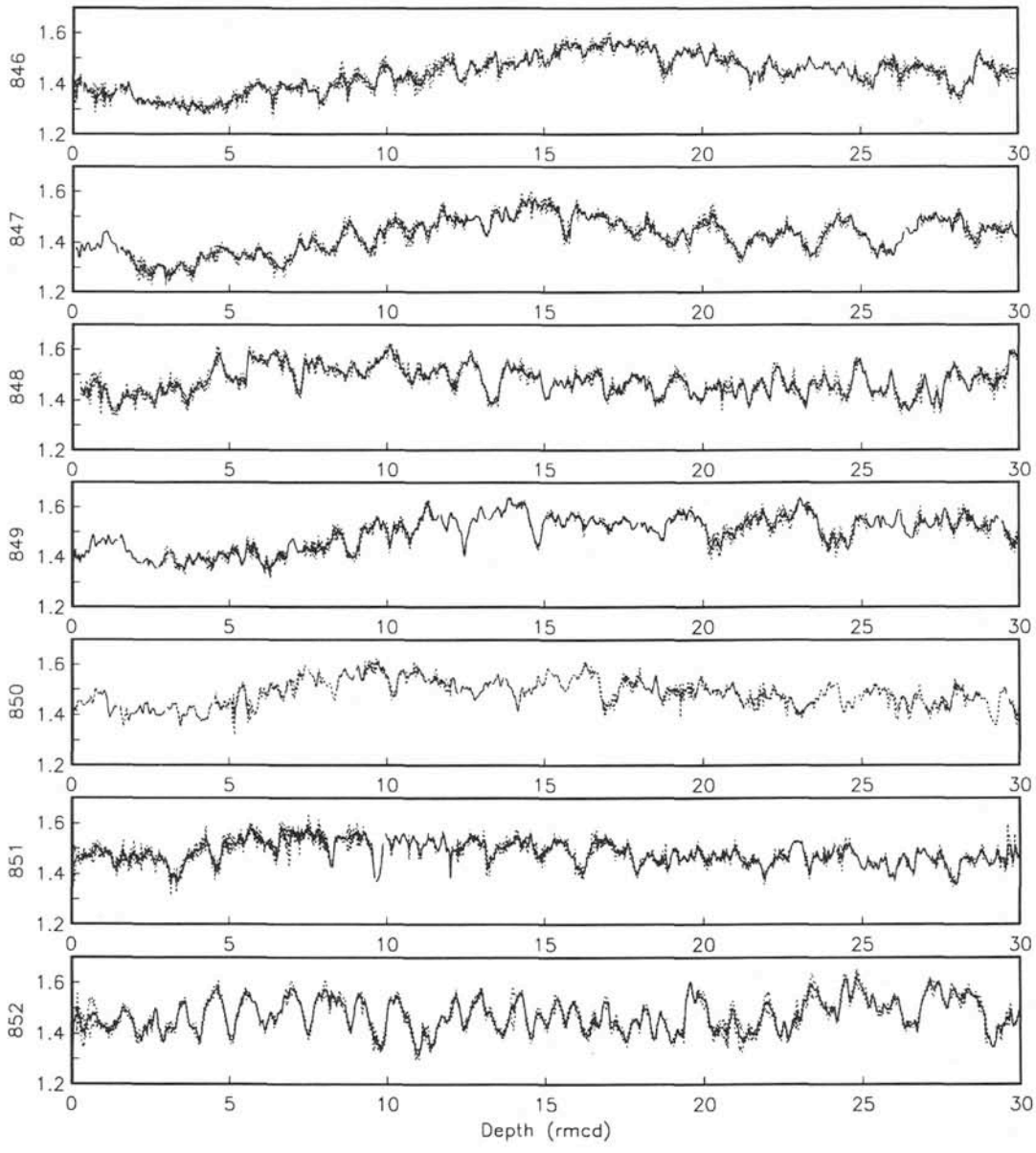


Figure 8. Stacked GRAPE records from Sites 846 to 852 with ±1 standard deviation envelopes (except for intervals where only one measurement is present). The 30-m sections shown are representative for each site.

A traditional one-way analysis of variance only yields information about whether a set of samples is statistically different from one another, with no information about how individual samples may differ. A modification of this traditional test known as Bonferroni's method (Rice, 1988) allows for a simultaneous comparison between individual pairs of measurements. From the seven sites, there are 21 possible pairwise comparisons. A set of simultaneous 95% confidence intervals for any two pairwise comparisons $Y_{i_1}$ and $Y_{i_2}$ is

$$(\overline{Y}_{i_1} - \overline{Y}_{i_2}) \pm s_p \frac{t_{18}(.025/21)}{\sqrt{J_i}}, \quad (1)$$

where $Y_{i_1}$ and $Y_{i_2}$ are the sample means, $t$ is the Bonferroni t statistic, $s_p$ is the square root of the pooled variance (= 0.0221), and $J$ is the average number of observations in each sample (3). The Bonferroni t statistic for an $\alpha = 0.05$ significance level in this case is $t_{18}(0.025/21) = 3.46$. Thus, if any two of the stacked GRAPE estimates from Sites 846 through 852 differ by more than 0.0441, they are significantly different from one another at the 0.05 level. Using this test, the Event F GRAPE maxima in Figure 9 are significantly different from one another, with the exception of four pairs of sites: 846/849, 847/849, 847/850, and 848/852. The remaining 17 possible pairwise comparisons are significantly different at the 0.05 level. Although this is an

**Table 4. Statistics for stacked GRAPE records from Sites 846 to 852 over GRAPE Event "F," defined by Shackleton et al. (1992).**

| Site | Event depth (rmcd) | GRAPE | *N* | Std. dev. |
|---|---|---|---|---|
| 846 | 145.27 | 1.621 | 4 | 0.031 |
| 847 | 117.41 | 1.571 | 5 | 0.011 |
| 848 | 36.60 | 1.409 | 4 | 0.015 |
| 849 | 101.47 | 1.605 | 4 | 0.016 |
| 850 | 76.16 | 1.533 | 2 | 0.008 |
| 851 | 69.12 | 1.463 | 2 | 0.041 |
| 852 | 41.72 | 1.367 | 4 | 0.025 |

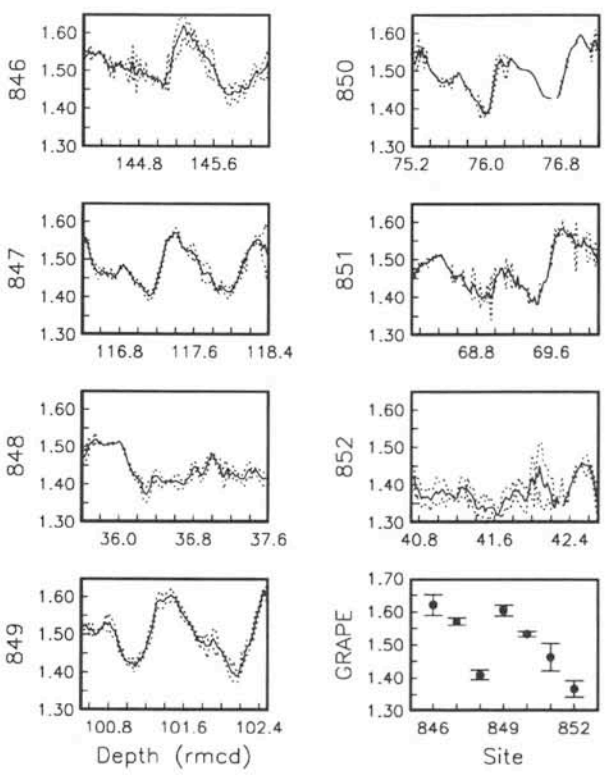


Figure 9. GRAPE Event F (defined by Shackleton, Crowhurst, et al., 1992) at Sites 846 through 852. Bottom right panel: mean and standard deviation of Event F (see Table 3 for depths).

analysis of only a single isolated GRAPE event, the implication from this example is that spatial differences in GRAPE data from site to site are statistically significant.

As illustrated in Figures 8 and 9, it is also possible to determine if adjacent peaks and valleys in the GRAPE records are significantly different from the surrounding features. At GRAPE Event F at Site 848, for example, the low amplitude peaks and troughs in the GRAPE record at 36.8 rmcd are within one standard deviation of each other. This is better illustrated in the portions of GRAPE records in Figure 8. Many large-scale events in the GRAPE records are prominent, but small amplitude variability often is within the range of the error bars. The implication from these data is that Sites 846 through 852 are characterized by significant within-site variability in wet-bulk density data as well as between-site variability. Thus, a spatial study of the GRAPE carbonate proxy records from these sites should resolve any variations in GRAPE densities that are significant.

## Depth Scale Variability

As noted by Ruddiman et al. (1987), were core breaks the only factor preventing recovery of continuous sedimentary sections, it would be straightforward to recover a continuous sedimentary section by drilling two adjacent holes offset in depth. However, the length of the drill string cannot be used as the only measure of positioning between holes. The cohesive properties of the sediment being cored introduce an additional degree of variability to coring recovery and coring gaps. Sediments having higher water content are likely to be more susceptible to coring disturbance. HPC design also has been suggested as a complicating factor, although no study has considered this explicitly.

Sea-state and heave of the vessel also are possible complicating factors. However, variability in coring gaps estimated from composite depth sections was compared with sea state and heave of vessel during Leg 138, and no clear relationship was seen (Hagelberg et al., 1992). This suggests that this effect alone is not the only process responsible for the presence of coring gaps.

Somehow, during the coring process, the sedimentary section must be expanded if core recovery is to be documented at 100%, yet the composite section suggests that more than 10% of the sequence is missing. Expansion of sediment caused by release of gas or release of overburden pressure has been suggested as a factor. Consolidation tests suggest that release of overburden pressure may account for up to ~33% of offset between composite and mbsf depths (MacKillop et al., this volume). Were compaction a significant process, then this might explain why only a portion of the true sedimentary sequence can be recovered. It appears that compaction effects may play a larger role in creating the apparent lack of complete recovery than previously thought. If so, then the remainder of coring variability may be accounted for by random changes in sea state, heave of vessel, and other coring artifacts.

## Local Variability in Sediment Deposition Rates

It is likely that some of the depth scale variability recorded in GRAPE measurements from hole to hole is related to heterogeneity in the sediment within a very small geographic area. Adjacent drilled holes typically are separated by tens of meters. Thus, the depth-scale variability that is resolved on within-core scales may also provide a measure of the natural variability in sedimentation rates. The inverse mapping methods used above for the first time provide a sufficient data set to examine the impact of this source of variability on geologic records.

Figure 10 presents the differences between the original (mcd) and revised composite depths (rmcd) for Sites 846 through 852 in histogram form. Only observations that were not part of the shipboard splice (the mapping reference) were included. The changes in depth from mcd to rmcd are roughly equally distributed about the mean, and the majority of measurements required less than a 10-cm change in depth. With the exception of Sites 846 and 848, almost all of the measurements at each hole at each site required changes in depth of less than 30 cm.

How much stretching or squeezing must occur between two successive measurements in one hole relative to another to correlate between the two? If this is determined, one can calculate the relative variability in sedimentation rates that is induced by the two factors of local differences in sedimentation and coring-related disturbance. The amount of variation in depth at small scales at a given site are determined by the correlation process. Converting to sedimentation rates, the range of sedimentation rate changes needed to account for between-hole differences can be compared to sedimentation rate changes that are imposed upon single records using time scale refinement strategies such as orbital tuning (e.g., Martinson et al., 1987).

For each hole at each mapped site (846 through 852), the differences in mcd between two successive downcore measurements were compared with the corresponding differences in revised mcd for the same pair of observations. Only measurements that were not part of the shipboard splice (reference signal) were included. In addition, since the average sampling interval for the GRAPE records was 1 to 2 cm, only observations that were originally less than 5-cm apart in mcd were included, because the idea is to determine a measure of the relative stretch or squeeze required between two initially adjacent observations. The measure of compression, $D$, is calculated as

$$D = \frac{MCD\,(i) - MCD\,(i-1)}{RMCD\,(i) - RMCD\,(i-1)} \qquad i = 1,2,3,\ldots \qquad (2)$$

$D$ calculated in this way measures the amount of compression between two successive points on the rmcd depth scale relative to the

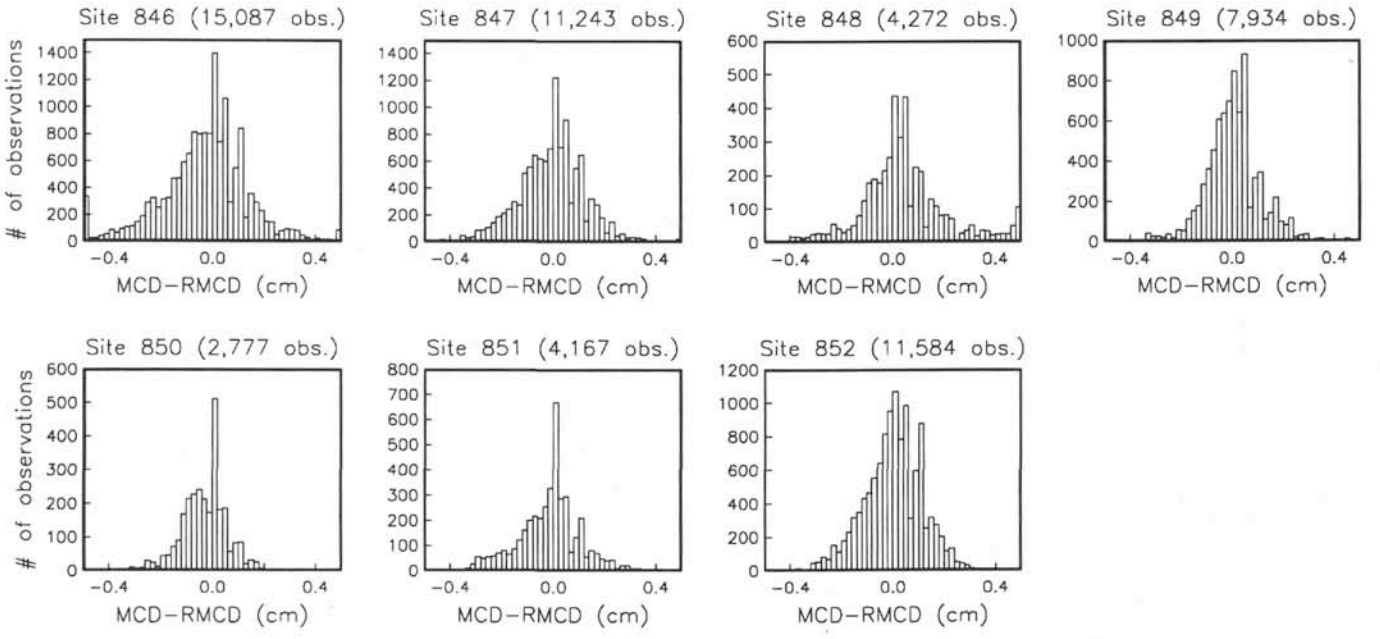


Figure 10. Differences between mcd and rmcd for each GRAPE measurement correlated to the shipboard splice using inverse correlation, Sites 846 through 852. These histograms indicate absolute differences between mcd depth and rmcd (intervals that are part of the shipboard splice have been excluded), and indicate that the bulk of changes between mcd and rmcd are 10 cm or less.

mcd depth scale. $D = 2.0$ indicates that successive measurements on the rmcd scale are compressed two times relative to the mcd scale, and $D = 0.5$ indicates that measurements on the rmcd scale are stretched two times relative to mcd depths. Table 5 gives the distribution of $D$, the amount of stretch or squeeze, as well as summary statistics for each site. $D$ is plotted as a function of depth for each hole in Site 852 in Figure 11.

As seen in Table 5, the amount of stretching ($D < 1$) and compression ($D > 1$) for each site is similar. For each site, the one standard deviation ranges are approximately $0.67 < D < 1.5$. Thus, the amount of distortion within a given core relative to a reference does not vary significantly from site to site, as measured using inverse correlation. This suggests three factors: (1) variation in the amplitudes of depth distortion is independent of sedimentation rate, as sites having a large range in sediment accumulation rates show the same level of distortion; (2) variation seen in small-scale variability may be an artifact of the coring process, because the depth scale changes are so similar from site to site; or (3) use of inverse correlation techniques to correlate at small scales has an inherent limitation in the number of Fourier coefficients that can be used, so that higher sedimentation rate sites are not correlated as well as lower sedimentation rate sites, and the result is that the amount of distortion appears similar.

It is likely that all three of these factors bear on the level of depth scale variability observed. Factor 3 can be partially ruled out as the number of Fourier coefficients used in inverse correlation rarely was the maximum, and the level of coherence between cores from adjacent holes was similar with both high and low sedimentation rate sites (Table 2). Factor 2 is difficult to address because the above measures of distortion are relative, that is the reference signal itself contains distortion due to coring variability. Although the resolution is lower, core-log integration may allow this factor to be addressed (e.g., Harris et al., this volume). As seen in Figure 11, although the *amplitude* of stretching and squeezing necessary to correlate at fine scale between adjacent holes is independent of sedimentation rate, the *rate of change of amplitudes* downcore is related to sedimentation rate.

If Factor 1 is true, then upper and lower limits on deposition rates within a given site can be estimated. Table 6 gives standard deviation and minimum and maximum sedimentation rates for each of Sites 846 through 852 (in the 0–5 ma range only for 847 through 852). Note (Table 5 and Fig. 10) that the bulk of measurements on the rmcd scale required no change ($D = 1.0$) between successive pairs, indicating relatively constant sedimentation rates measured from adjacent holes (Fig. 11). At Site 847, for example, out of 10,671 total pairs of observations, $D$ fell between 0.5 and 0.7 (50% stretch) for only 1375 pairs, and $D$ fell between 1.9 and 2.3 (50% compression) for 1073 pairs.

The extremes of sedimentation rate variability induced solely by this interhole variability are illustrated in the following example from Site 847. The highest sedimentation rate recorded at Site 847 is 66.7 mcd/m.y., and the lowest sedimentation rate is 15.5 mcd/m.y. (Table 6; Shackleton, Crowhurst, et al., 1992). The extremes of stretching

**Table 5. Frequency distributions of $D^a$ for initially adjacent GRAPE measurements.**

| Site | Total no. pairs | Mean | Std. dev. | Range |
|---|---|---|---|---|
| 846 | 14,634 | 1.15 | 0.52 | 0.09–4.00 |
| 847 | 10,671 | 1.07 | 0.40 | 0.20–3.99 |
| 848 | 4,084 | 1.10 | 0.40 | 0.25–3.00 |
| 849 | 7,589 | 1.05 | 0.39 | 0.20–3.00 |
| 850 | 2,622 | 1.07 | 0.41 | 0.33–3.00 |
| 851 | 3,760 | 1.10 | 0.44 | 0.20–5.00 |
| 852 | 10,896 | 1.10 | 0.47 | 0.14–3.00 |

| | No. of observations | | | | | | |
|---|---|---|---|---|---|---|---|
| $D$ | Site 846 | Site 847 | Site 848 | Site 849 | Site 850 | Site 851 | Site 852 |
| 0.1–0.3 | 66 | 27 | 2 | 4 | 0 | 7 | 20 |
| 0.3–0.5 | 374 | 200 | 39 | 185 | 78 | 65 | 335 |
| 0.5–0.7 | 2011 | 1375 | 443 | 1002 | 337 | 317 | 1596 |
| 0.7–0.9 | 633 | 475 | 183 | 295 | 97 | 556 | 231 |
| 0.9–1.1 | 7692 | 6873 | 2651 | 4997 | 1666 | 1733 | 6608 |
| 1.1–1.5 | 522 | 283 | 136 | 189 | 70 | 611 | 180 |
| 1.5–1.9 | 521 | 307 | 151 | 187 | 72 | 242 | 242 |
| 1.9–2.3 | 2249 | 1073 | 463 | 685 | 290 | 158 | 1565 |
| 2.3–2.7 | 3 | 0 | 0 | 0 | 0 | 9 | 0 |
| 2.7–3.1 | 292 | 57 | 16 | 45 | 12 | 44 | 119 |
| 3.1–3.5 | 0 | 0 | 0 | 0 | 0 | 0 | 0 |
| 3.5–3.9 | 0 | 0 | 0 | 0 | 0 | 0 | 0 |
| 3.9–4.1 | 0 | 1 | 0 | 0 | 0 | 18 | 0 |

[a] $D$ = change in mcd/change in rmcd.

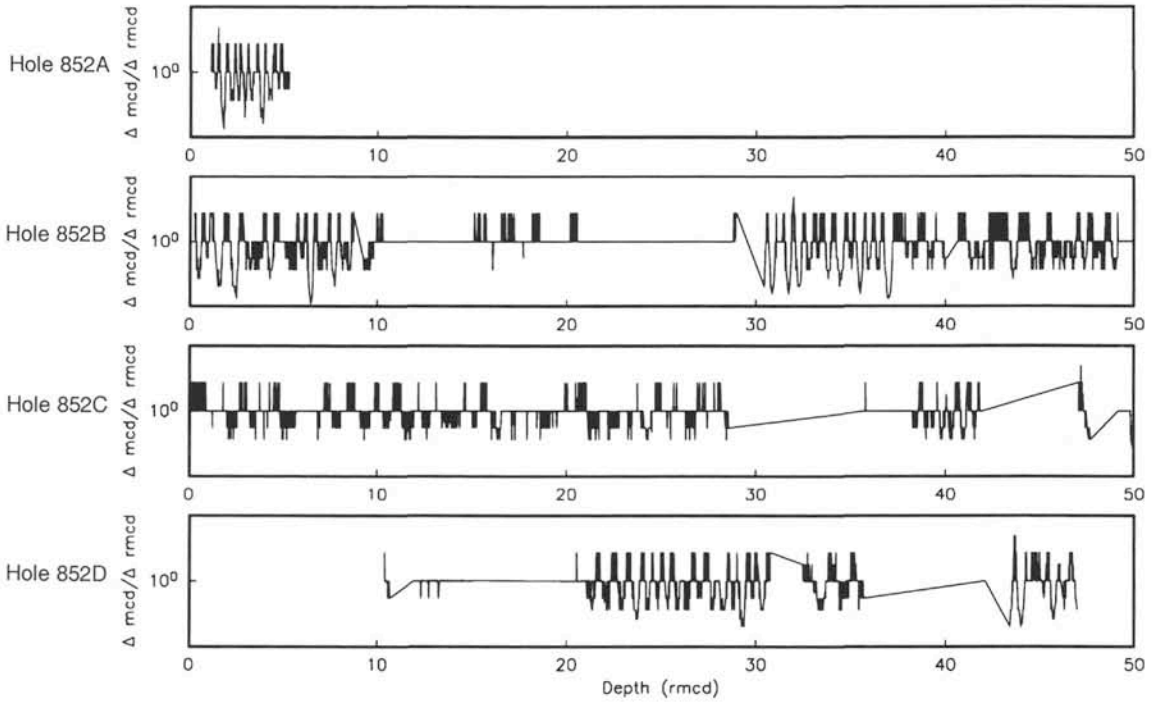


Figure 11. $D$ (see text and Table 5) as a function of rmcd for each hole at Site 852. $D = 1$ indicates no relative stretch or squeeze between a pair of observations going from mcd to rmcd; $D > 1$ indicates that the pair of observations are closer together on the rmcd scale relative to the mcd scale. $D < 1$ indicates that the pair of observations must be stretched on the rmcd scale relative to the mcd to fit the reference.

and squeezing estimated by $D$ for Site 847 are $D = 0.20$, indicating a five-fold stretching of the rmcd scale relative to mcd and $D = 3.99$, indicating a four-fold compression of rmcd relative to mcd (Table 5). These $D$ values are used to estimate maximum and minimum sedimentation rate changes that might be induced purely by interhole stretching and squeezing. The maximum possible sedimentation rate is 66.6 mcd/m.y. divided by 0.20, (the maximum stretch for Site 847), or 335 mcd/m.y. The minimum possible sedimentation rate related to compression is 15.5 mcd/m.y. divided by 3.99, (the maximum compression for Site 847), or 3.9 mcd/m.y. (Table 6). By comparison, the orbitally calibrated shipboard chronology developed for Site 847 (Shackleton, Crowhurst, et al., 1992) has a maximum sedimentation rate of 125 mcd/m.y. and a minimum of 11.9 mcd/m.y., a range which fits within the range of distortion-related sedimentation extremes (Table 6).

Potential sedimentation rate changes for Sites 846 through 852 that are induced by interhole correlation alone are compared to sedimentation rate changes induced by orbital time-scale calibration in Table 6. Applying the values for the mean, variance, and range of $D$ (Table 5) to the shipboard sedimentation rate statistics (Table 6) produces a set of sedimentation rate extremes (Table 6). These values indicate that significant changes in sedimentation rates are required simply to correlate between adjacent holes. These values can be compared to the sedimentation rate changes in the orbitally tuned chronology given in Table 6 (Shackleton, Crowhurst, et al., 1992). In all cases, the extremes of the tuned time scale are within the level of variability that would be predicted solely on the basis of stretching and squeezing between adjacent holes.

This exercise makes the important point that the degree of variability present in tuned sedimentation rate models is no greater than the variability induced by the compression and stretching required to map adjacent holes to one another at high resolution. While this does not have direct bearing on determining what the true range of sedimentation rate variability is, large differences in sedimentation rate between tuned (Shackleton, Crowhurst, et al., 1992) and untuned (Mayer, Pisias, Janecek, et al., 1992) chronologies cannot be discounted on this basis, as the range of sedimentation rate variability fits easily within the range of intrasite core distortion.

## CONCLUSIONS

Very high-resolution correlations between adjacent holes at sites drilled during Leg 138 are possible. A revised composite depth section accurate to the order of centimeters places data from multiple holes onto a common depth scale. Correlations between holes based on GRAPE bulk density measurements were confirmed by comparing these data with color reflectance and magnetic susceptibility data. The measurements in each hole can be stacked to arrive at a less noisy GRAPE estimate for each 2-cm depth at each site. The stacking exercise increases the signal/noise ratio. The stacking exercise produces a site-representative record of GRAPE bulk density that uses all of the available data at a given site, and that can be used for high-resolution paleoceanographic study. A quantitative estimate of error for the GRAPE amplitudes is obtained from the multiple measurements at every depth. The high-resolution correlations among adjacent holes can be used to assess the amount of distortion required to map three adjacent holes to one another. This has implications for small-scale sedimentation rate variability at a given site. Sedimentation rates in the tuned chronology of Shackleton et al. (1992a) relative to the shipboard chronology are entirely within the range of variability predicted from correlating among adjacent holes in the depth domain.

## ACKNOWLEDGMENTS

We thank the Leg 138 Scientific Party, particularly T. Janecek, D.A. Schneider, M. Lyle, and J. Farrell for discussion regarding composite depths, coring offsets, correlation strategies, and related

**Table 6. Sedimentation rate statistics, Sites 846 through 852 (from Mayer, Pisias, Janecek, et al., 1992).**[a]

| Site | Mean | ±1 Std. dev. | Mininum rate[b] | Maximum rate |
|---|---|---|---|---|
| 846 | 33.2 | 15.0–51.5 | 5.5 | 61.3 |
| 847 | 36.7 | 21.7–51.7 | 15.5 | 66.7 |
| 848 | 12.2 | 6.3–18.1 | 5.2 | 21.2 |
| 849 | 41.9 | 21.5–62.3 | 25.8 | 75.5 |
| 850 | 33.3 | 16.3–50.3 | 18.0 | 64.2 |
| 851 | 26.2 | 15.8–36.6 | 18.8 | 48.1 |
| 852 | 14.1 | 10.3–17.9 | 9.1 | 20.6 |

Statistics of predicted minimum and maximum sedimentation rates from data above that would be produced by compression and stretching between adjacent cores, as indicated by *D* (Table 5).

| Site | Mean | ±1 Std. dev.[c] | Minimum rate | Maximum rate |
|---|---|---|---|---|
| 846 | 28.9 | 8.9–81.7 | 1.4 | 674.3 |
| 847 | 34.2 | 14.8–77.2 | 3.9 | 335.2 |
| 848 | 11.1 | 4.2–25.9 | 1.7 | 84.8 |
| 849 | 39.9 | 14.9–94.4 | 8.6 | 377.5 |
| 850 | 31.1 | 11.0–76.2 | 6.0 | 194.5 |
| 851 | 23.8 | 10.2–55.4 | 3.8 | 240.5 |
| 852 | 12.8 | 6.6–28.4 | 3.0 | 147.1 |

Range in the maximum/minimum sedimentation rates from the tuned chronology for Sites 846 through 852 (Shackleton et al., this volume). Compare to predicted values above.

| Site | Mean | ±1 Std. dev. | Minimum rate | Maximum rate |
|---|---|---|---|---|
| 846 | 41.0 | 25.5–56.5 | 11.4 | 121.2 |
| 847 | 35.3 | 19.5–51.1 | 11.9 | 124.9 |
| 848 | 10.4 | 5.0–15.8 | 1.9 | 36.4 |
| 849 | 36.2 | 11.9–60.5 | 9.0 | 199.9 |
| 850 | 28.5 | 7.5–49.5 | 6.9 | 210.0 |
| 851 | 22.4 | 10.1–34.7 | 7.9 | 72.2 |
| 852 | 12.3 | 7.5–17.1 | 4.8 | 31.5 |

[a]Over the interval 0–5 m.y. only for Sites 847 through 852.
[b]Rates are in mcd/m.y.
[c]The standard deviations in this section of Table 6 were calculated by applying the standard deviation of *D* (Table 5) to the sedimentation rate standard deviation given in the top section of Table 6.

issues. W.F. Ruddiman, P. deMenocal, and J. Alexandrovich provided useful reviews of the manuscript. A JOI-USSAC Ocean Drilling Fellowship to T. Hagelberg supported development of the compositing techniques that were used during Leg 138 and the additional development presented here. This study was supported by NSF grant OCE-9216929 to N. Pisias and T. Hagelberg.

## REFERENCES*

Alexandrovich, J.M., and Hays, J.D., 1989. High-resolution stratigraphic correlation of ODP Leg 111 Holes 677A and 677B and DSDP Leg 69 Hole 504. *In* Becker, K., Sakai, H., et al., *Proc. ODP, Sci. Results,* 111: College Station, TX (Ocean Drilling Program), 263–276.

Bloemendal, J., Tauxe, L., Valet, J.-P., and Shipboard Scientific Party, 1988. High-resolution, whole-core magnetic susceptibility logs from Leg 108. *In* Ruddiman, W., Sarnthein, M., Baldauf, J., et al., *Proc. ODP, Init. Repts.,* 108: College Station, TX (Ocean Drilling Program), 1005–1013.

Boyce, R.E., 1976. Definitions and laboratory techniques of compressional sound velocity parameters and wet-water content, wet-bulk density, and porosity parameters by gravimetric and gamma ray attenuation techniques. *In* Schlanger, S.O., Jackson, E.D., et al., *Init. Repts. DSDP,* 33: Washington (U.S. Govt. Printing Office), 931–958.

deMenocal, P., Bloemendal, J., and King, J., 1991. A rock-magnetic record of monsoonal dust deposition to the Arabian Sea: evidence for a shift in the mode of deposition at 2.4 Ma. *In* Prell, W.L., Niitsuma, N., et al., *Proc. ODP, Sci. Results,* 117: College Station, TX (Ocean Drilling Program), 389–407.

Farrell, J.W., and Janecek, T.R., 1991. Late Neogene paleoceanography and paleoclimatology of the northeast Indian Ocean (Site 758). *In* Weissel, J., Peirce, J., Taylor, E., Alt, J., et al., *Proc. ODP, Sci. Results,* 121: College Station, TX (Ocean Drilling Program), 297–358.

Froelich, P.N., Malone, P.N., Hodell, D.A., Ciesielski, P.F., Warnke, D.A., Westall, F., Hailwood, E.A., Nobes, D.C., Fenner, J., Mienert, J., Mwenifumbo, C.J., and Müller, D.W., 1991. Biogenic opal and carbonate accumulation rates in the subantarctic South Atlantic: the late Neogene of Meteor Rise Site 704. *In* Ciesielski, P.F., Kristoffersen, Y., et al., *Proc. ODP, Sci. Results,* 114: College Station, TX (Ocean Drilling Program), 515–550.

Gardner, J.V., 1982. High-resolution carbonate and organic-carbon stratigraphies for the late Neogene and Quaternary from the western Carribbean and eastern equatorial Pacific. *In* Prell, W.L., Gardner, J.V., et al., *Init. Repts. DSDP,* 68: Washington (U.S. Govt. Printing Office), 347–364.

Hagelberg, T., Shackleton, N., Pisias, N., and Shipboard Scientific Party, 1992. Development of composite depth sections for Sites 844 through 854. *In* Mayer, L., Pisias, N., Janecek, T., et al., *Proc. ODP, Init. Repts.,* 138 (Pt. 1): College Station, TX (Ocean Drilling Program), 79–85.

Hays, J.D., Saito, T., Opdyke, N.D., and Burckle, L.R., 1969. Pliocene-Pleistocene sediments of the equatorial Pacific: their paleomagnetic, biostratigraphic, and climatic record. *Geol. Soc. Am. Bull.,* 80:1481–1513.

Heath, G.R., Rea, D.H., and Levi, S., 1985. Paleomagnetism and accumulation rates of sediments at Sites 576 and 578, Deep Sea Drilling Project Leg 86, western North Pacific. *In* Heath, G.R., Burckle, L.H., et al., *Init. Repts. DSDP,* 86: Washington (U.S. Govt. Printing Office), 459–502.

Karlin, K., Ruddiman, W.F., and McIntyre, A., 1989. Comparison of late Pliocene and late Pleistocene sea-surface temperatures of the equatorial Atlantic divergence. *In* Ruddiman, W., Sarnthein, M., et al., *Proc. ODP, Sci. Results,* 108: College Station, TX (Ocean Drilling Program), 187–210.

Kent, D.V., and Spariosu, D.J., 1982. Magnetostratigraphy of Caribbean Site 502 hydraulic piston cores. *In* Prell, W.L., Gardner, J.V., et al., *Init. Repts. DSDP,* 68: Washington (U.S. Govt. Printing Office), 419–433.

Martinson, D.G., Menke, W., and Stoffa, P.L., 1982. An inverse approach to signal correlation. *J. Geophys. Res.,* 87:4807–4818.

Martinson, D.G., Pisias, N.G., Hays, J.D., Imbrie, J., Moore, T.C., Jr., and Shackleton, N.J., 1987. Age dating and the orbital theory of the ice ages: development of a high-resolution 0 to 300,000-year chronostratigraphy. *Quat. Res. (N.Y.),* 27:1–29.

Mayer, L., Pisias, N., Janecek, T., et al., 1992. *Proc. ODP, Init. Repts.,* 138 (Pts. 1 and 2): College Station, TX (Ocean Drilling Program).

Mayer, L.A., 1980. Deep-sea carbonates: physical property relationships and the origin of high-frequency acoustic reflectors. *Mar. Geol.,* 38:165–183.

———, 1991. Extraction of high-resolution carbonate data for paleoclimate reconstruction. *Nature,* 352:148–150.

Mayer, L.A., Shipley, T.H., and Winterer, E.L., 1986. Equatorial Pacific seismic reflectors as indicators of global oceanographic events. *Science,* 233:761–764.

Mix, A.C., Rugh, W., Pisias, N.G., Veirs, S., Leg 138 Shipboard Sedimentologists (Hagelberg, T., Hovan, S., Kemp, A., Leinen, M., Levitan, M., Ravelo, C.), and Leg 138 Scientific Party, 1992. Color reflectance spectroscopy: a tool for rapid characterization of deep-sea sediments. *In* Mayer, L., Pisias, N., Janecek, T., et al., *Proc. ODP, Init. Repts.,* 138 (Pt. 1): College Station, TX (Ocean Drilling Program), 67–77.

Murray, D.W., and Prell, W.L., 1991. Pliocene to Pleistocene variations in calcium carbonate, organic carbon, and opal on the Owen Ridge, northern Arabian Sea. *In* Prell, W.L., Niitsuma, N., et al., *Proc. ODP, Sci. Results,* 117: College Station, TX (Ocean Drilling Program), 343–363.

Preistley, M.B., 1988. *Spectral Analysis and Time Series:* London (Academic).

Prell, W.L., Gardner, J.V., et al., 1982. *Init. Repts. DSDP,* 68: Washington (U.S. Govt. Printing Office).

Raymo, M.E., Ruddiman, W.F., Backman, J., Clement, B.M., and Martinson, D.G., 1989. Late Pliocene variation in Northern Hemisphere ice sheets and North Atlantic deep water circulation. *Paleoceanography,* 4:413–446.

Rice, J.A., 1988. *Mathematical Statistics and Data Analysis:* Pacific Grove, CA (Wadsworth and Brooks/Cole).

Robinson, S.G., 1990. Applications for whole-core magnetic susceptibility measurements of deep-sea sediments: Leg 115 results. *In* Duncan, R.A., Backman, J., Peterson, L.C., et al., *Proc. ODP, Sci. Results,* 115: College Station, TX (Ocean Drilling Program), 737–771.

Ruddiman, W., Sarnthein, M., Baldauf, J., et al., 1988, *Proc. ODP, Init. Repts.,* 108 (Sections 1 and 2): College Station, TX (Ocean Drilling Program).

Ruddiman, W.F., Cameron, D., and Clement, B.M., 1987. Sediment disturbance and correlation of offset holes drilled with the hydraulic piston corer:

*Abbreviations for names of organizations and publication titles in ODP reference lists follow the style given in *Chemical Abstracts Service Source Index* (published by American Chemical Society).

Leg 94. *In* Ruddiman, W.F., Kidd, R.B., Thomas, E., et al., *Init. Repts. DSDP,* 94 (Pt. 2): Washington (U.S. Govt. Printing Office), 615–634.

Ruddiman, W.F., Raymo, M.E., Martinson, D.G., Clement, B.M., and Backman, J., 1989. Pleistocene evolution: Northern Hemisphere ice sheets and North Atlantic Ocean. *Paleoceanography,* 4:353–412.

Shackleton, N.J., Berger, A., and Peltier, W.R., 1990. An alternative astronomical calibration of the lower Pleistocene time scale based on ODP Site 677. *Trans. R. Soc. Edinburgh, Earth Sci.,* 81:251–261.

Shackleton, N.J., Crowhurst, S.J., Pisias, N.G., Hagelberg, T.K., Schneider, D.A., Mix, A.C., and ODP Leg 138 Shipboard Party, 1992. An astronomically calibrated Pliocene time scale based on Leg 138 GRAPE density records. *Proc. Fourth Int. Conf. on Paleoceanography,* Kiel, Germany, 240. (Abstract)

Shackleton, N.J., and Hall, M.A., 1983. Stable isotope record of Hole 504 sediments: high-resolution record of the Pleistocene. *In* Cann, J.R., Langseth, M.G., Honnorez, J., Von Herzen, R.P., White, S.M., et al. *Init. Repts. DSDP,* 69:431–441.

———, 1989. Stable isotope history of the Pleistocene at ODP Site 677. *In* Becker, K., Sakai, H., et al., *Proc. ODP, Sci. Results,* 111: College Station, TX (Ocean Drilling Program), 295–316.

Shackleton, N.J., Hall, M.A., and Bleil, U., 1985. Carbon-isotope stratigraphy, Site 577. *In* Heath, G.R., Burckle, L.H., et al., *Init. Repts. DSDP,* 86: Washington (U.S. Govt. Printing Office), 503–511.

Shackleton, N.J., and Shipboard Scientific Party, 1992. Sedimentation rates: toward a GRAPE density stratigraphy for Leg 138 carbonate sections. *In* Mayer, L., Pisias, N., Janecek, T., et al., *Proc. ODP, Init. Repts.,* 138 (Pt. 1): College Station, TX (Ocean Drilling Program), 87–91.

**Date of initial receipt: 1 February 1993**
**Date of acceptance: 28 December 1993**
**Ms 138SR-103**